GEOLOGY

Mediterranean radiocarbon offsets and calendar dates for prehistory

Sturt W. Manning[1]*, Bernd Kromer[2], Mauro Cremaschi[3], Michael W. Dee[4], Ronny Friedrich[5], Carol Griggs[1], Carla S. Hadden[6]

Copyright © 2020 The Authors, some rights reserved; exclusive licensee American Association for the Advancement of Science. No claim to original U.S. Government Works. Distributed under a Creative Commons Attribution NonCommercial License 4.0 (CC BY-NC).

A single Northern Hemisphere calibration curve has formed the basis of radiocarbon dating in Europe and the Mediterranean for five decades, setting the time frame for prehistory. However, as measurement precision increases, there is mounting evidence for some small but substantive regional (partly growing season) offsets in same-year radiocarbon levels. Controlling for interlaboratory variation, we compare radiocarbon data from Europe and the Mediterranean in the second to earlier first millennia BCE. Consistent with recent findings in the second millennium CE, these data suggest that some small, but critical, periods of variation for Mediterranean radiocarbon levels exist, especially associated with major reversals or plateaus in the atmospheric radiocarbon record. At high precision, these variations potentially affect calendar dates for prehistory by up to a few decades, including, for example, Egyptian history and the much-debated Thera/Santorini volcanic eruption.

INTRODUCTION

Relevance of IntCal to the Mediterranean

Since the late 1960s, the principal basis for a calendar time scale for pre- and protohistoric archaeology in the Northern Hemisphere (NH) is via radiocarbon (^{14}C) dating, with specific calendar age estimates for objects, contexts, sites, and cultures derived from comparison of measured ^{14}C dates with a common NH radiocarbon calibration curve. In consequence, considerable effort focuses on the development of an increasingly accurate and long ^{14}C calibration curve for the NH (*1*–*4*). The general assumption of the field is that for the midlatitudes of the NH, rapid atmospheric mixing should make a single ^{14}C calibration curve suitable, allowing for stated errors, for the entire hemisphere (*2*–*6*). Within noisy data, a north-south gradient in ^{14}C values is recognized (*5*–*9*), but this is considered small, static, and largely irrelevant for the midlatitudes (>30°N and <60°/70°N). At midlatitudes, trees with similar growing seasons, even if at differing latitudes, typically exhibit little substantive offset (*5*, *8*, *10*). Hence, a single NH ^{14}C calibration curve (IntCal), constructed mainly from known-age wood from central and northern Europe and North America, has become the basis for calendar dates for pre- and protohistory and for other work requiring an accurate absolute time scale (*1*–*4*). This calibration curve is assumed as relevant for everywhere in the midlatitudes of the NH, including the Mediterranean, home of "Old World" prehistory. Intercomparisons between laboratories invariably indicate measurement noise, but typically, this is approximately around the consensus calibration curve values (*11*), and data from the same laboratory for tree rings from mid-NH locations with similar growing seasons usually compare closely to each other and the consensus IntCal values [e.g., the three Heidelberg (Hd) datasets in Fig. 1A]. In recent years, some time series of ^{14}C measurements on dendrochronologically dated wood have been reported, indicating small offsets between the reporting laboratory and IntCal for various intervals (*10*, *12*, *13*), but the assumption has been that there is either a small laboratory offset or the need to correct (improve) IntCal. The notion of an underlying globally valid midlatitude NH calibration curve has remained.

However, data measurements in recent years challenge this convenient belief. Various small offsets in contemporary (same calendar years) ^{14}C levels are reported for known-age plant material from several areas, including the Mediterranean (*8*, *13*–*19*). Since these variations occur even within similar latitude groupings (*8*), factors other than mere latitude [while a partial component (*6*–*8*)] must be involved, with differences in growing seasons or climate processes linked with solar and ocean systems suggested. Differences in growing season are potentially relevant, as an intra-annual pattern in transport across the extratropical tropopause leads to an observed natural seasonal variation in midlatitude NH tropospheric ^{14}C levels between a winter/spring low (minimum late March to early April) and a summer to early autumn high (peak mid-September) (*15*, *19*–*22*). To date, these typically modest variations have not been regarded as undermining the general use of a common calibration curve for the entire hemisphere. The partial exception is Egypt, where an offset allowance of 19 ± 5 ^{14}C years was proposed (*16*, *23*) and appears necessary to achieve plausible protohistoric dates (*23*, *24*). For Egypt, the small regional offset was assumed to be constant through time, but even this assumption is challenged. Two episodes of substantial ^{14}C offsets have been observed through comparisons of measurements on known-age wood from southern Jordan versus the record from central and northern Europe. These offsets appear episodic and, hence, not amenable to the application of a simple constant offset or error enlargement (*18*). However, the limiting factor in a number of the cases where offsets or differences are reported is the problem that, partly because they are so small, we cannot always discern the sources of variability, for example, interlaboratory variations in methods and instruments (*1*–*4*, *10*, *12*), versus real differences in ^{14}C levels from contemporary samples. For example, in earlier works, ^{14}C ages for high-elevation bristlecone pine (BCP) measured at Arizona (AA) consistently tended to be older than ^{14}C ages for contemporary

[1]Cornell Tree Ring Laboratory, Department of Classics, B-48 Goldwin Smith Hall, Cornell University, Ithaca, NY 14853, USA. [2]Institute of Environmental Physics, University of Heidelberg, D-69120 Heidelberg, Germany. [3]Dipartimento di Scienze della Terra "Ardito Desio," Università degli Studi di Milano, Via Festa del Perdono 7, 20122 Milano, Italy. [4]Centre for Isotope Research, Faculty of Science and Engineering, University of Groningen, Nijenborgh 6, NL-9747 AG Groningen, Netherlands. [5]Curt-Engelhorn-Center Archaeometry gGmbH, 68159 Mannheim, Germany. [6]Center for Applied Isotope Studies, University of Georgia, 120 Riverbend Rd., Athens, GA 30602, USA.
*Corresponding author. Email: sm456@cornell.edu

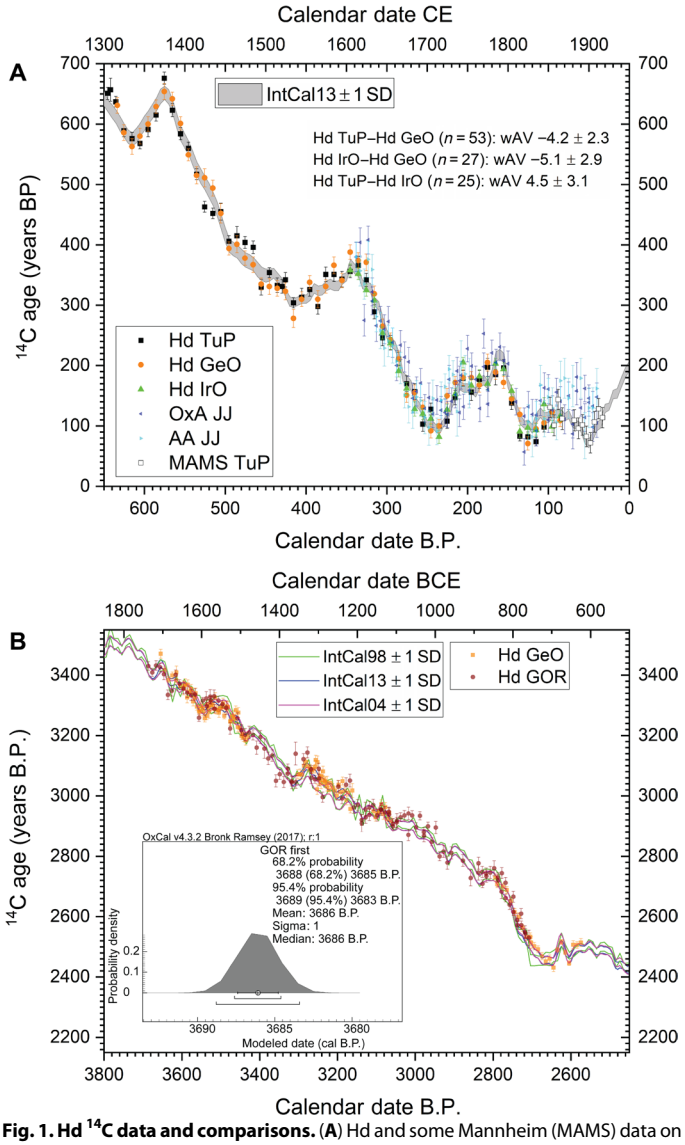

Fig. 1. Hd ^{14}C data and comparisons. (**A**) Hd and some Mannheim (MAMS) data on known-age Turkish pine (TuP), German oak (GeO), and Irish oak (IrO) (table S1) compared with the IntCal13 calibration curve (*4*) and Oxford (OxA) and Arizona (AA) data on Jordan juniper (JJ) (*18*). Calendar dates B.P. (before the present) (from 1950 CE) are shown. The differences [weighted averages (wAV)] in ^{14}C age between the pairs of data from time series of similar blocks of tree rings with the same midpoint age from GeO, high-elevation TuP, and IrO all measured at Hd are shown. All error bars shown and band width are 1 SD. (**B**) Hd Gordion (GOR) juniper data compared with Hd GeO for the second to first millennia BCE (1 SD error bars) and placed against the IntCal98 (*1*), IntCal04 (*2*), and IntCal13 calibration curves (1 SD) (*4*). The inset shows the "wiggle-match" fit of the tree ring sequenced Hd GOR dataset versus IntCal04 using OxCal (*39*); the best fit is the same against IntCal98 (*1*) and 1 year older versus IntCal13 (*4*).

low-elevation NH tree rings (*2*, *14*, *25*). Some laboratory intercomparisons, including remeasurement of BCP, primarily suggested a laboratory offset issue, but other work including a parallel dating of BCP and Irish oak (IrO) at Belfast indicated consistently older (41 ± 9.2 ^{14}C years) ^{14}C ages for the BCP (*2*, *14*, *25*). Overall, a limitation for the field is that only a few groups have performed suitable experiments over longer time periods under the same laboratory conditions to resolve seasonal, or regional (growing season), or similar NH latitudinal differences (*6*, *8*, *10*, *12*, *14*, *15*, *17*, *26*, *27*).

The Jordanian and Egyptian cases (*16*, *18*, *23*) suggest that a recurring Mediterranean region offset, versus just a few special cases exhibiting impacts of major solar minima or large-scale climate change (*15*, *17*), applies typically only for plants with growing seasons substantially offset from those standard in central and northern Europe (e.g., winter to early/earlier summer versus spring through the entire summer). This is typical of plants in many areas of the lower- to moderate-elevation Mediterranean growing under either Mediterranean or continental conditions, with rainfall/snow in autumn, winter, and spring, and growth limited by hot, dry summers (*18*, *28*). We might therefore assume that the instances of substantive offsets, of relevance, occur especially under circumstances that stretch the normal differences in the growing seasons of plants. One scenario observed is that warmer and drier conditions in the northern Mediterranean, such as those associated with positive phases of the North Atlantic Oscillation (NAO), advance the start of the Mediterranean growing season (*29*). These circumstances potentially exacerbate an offset with central and northern Europe, where, typically, a positive NAO will lead to warmer temperatures and increased moisture availability (*30*) and, hence, a potentially lengthened later summer to beginning of autumn growth period. Another scenario that is likely of interest is when there is increased moisture availability and mild climatic conditions in the Mediterranean, as observed in some recent periods following major reversals in the ^{14}C record (*18*, *31*, *32*), which could again extend and hence exaggerate existing growing season differences (*15*, *16*, *18*). For species and contexts where temperature is the critical threshold for triggering spring growth, such as deciduous oaks (*33*), circumstances that stretch and increase (or the reverse) differentiation in the timing of the temperature initiation threshold between Mediterranean contexts, versus those in central and northern Europe, which can then also affect—that is, bring forward—the end of the growth period (via very dry–to–drought conditions) (*34*), will be especially relevant. In reverse, the observations of periods of regionally applicable ^{14}C offsets could become a potential indicator of medium-frequency climate-earth system processes (or intersections of these processes).

The focus on differences between growing seasons, versus simply latitude, is highlighted by considering a Mediterranean case, which does not have a lower-elevation Mediterranean growing season. Turkish pine (*Pinus nigra*) from Çatacık in western Turkey grows in a high-elevation context where very cold winters create spring-summer growing conditions and timings (*35*) similar to central and northern Europe. Radiocarbon measurements on wood from these trees (*19*, *27*) thus usually show no apparent offset in the periods of reversals and plateaus in the ^{14}C calibration record that were identified in the Jordanian juniper time series (~1685 to 1762 CE and 1818 to 1912 CE) (Fig. 1A) (*18*). This negative case observation indicates the relevance of specific growing season differences—where present, as in the Jordan example—above, and beyond, the small latitudinal gradient recognized in ^{14}C values (*5*–*8*).

Differences in typical growing season and ^{14}C offsets

The potential importance of a diverging (i.e., intra-annual temporally offset) growing season for lower-elevation regions with a typical Mediterranean climate for archaeology is self-evident: Most of the major historical and archaeological centers in the Mediterranean lie in lower-elevation settings governed by such a typical Mediterranean

climate regime. Therefore, the issue of potential growing season–related recurring ^{14}C offset episodes is relevant to high-precision dating in Old World archaeology and creates the potential for some small but key ^{14}C calibration "fault line" episodes between parts of the Mediterranean Old World versus central and northern Europe. This is an important issue as numerous research groups continually push for, and rely on, ever higher-precision Mediterranean archaeological chronologies. The field also needs to reorient: The issue is not to adjust IntCal (both current and the forthcoming IntCal20). Rather, a single "standard" ^{14}C calibration curve built from midlatitude and spring and especially summer growing season–dominated wood (i.e., IntCal) cannot be fully representative, at high resolution, of the Mediterranean at those times when a growing season offset appears to operate at measurable and substantive scale. This contradiction is highlighted in recent work. A report of an offset at ~1660 to 1540 BCE between new AA accelerator mass spectrometry (AMS) ^{14}C measurements on BCP and IrO versus the existing IntCal13 dataset is stated as directly relevant to the Mediterranean (*13*), with the authors writing that

> "The bristlecone pine samples represent a c. 45 day growth season from mid to late June until late July or early August, with limited potential for photosynthesis outside the growing season. The oak latewood samples represent late May/June. Together, they represent the main growth season in the Mediterranean."

However, the growing seasons for this wood are not, in fact, coeval with the typical lower-elevation Mediterranean growing season. As stated in the quote, BCP tree ring growth occurs from mid to late June until late July or early August (*13*). This is mostly after the traditional autumn-winter-spring lower-elevation Mediterranean growing season for many field crops (assuming no irrigation). For autumn/winter-sown crops in the Mediterranean—such as (most) barley, wheat, oats, peas, lentils, and vetch—the traditional harvest dates vary by latitude and elevation. Harvest is earlier in lower-elevation southern areas, e.g., April to May (Jordan and Israel) or May to June (Cyprus and lowland Crete and lower elevations in north Africa and southern Spain), whereas it is later in northern or higher areas—e.g., lowland north Greece harvest is from June to early July, and in the mountains of northwest Greece, it occurs even later, and it is June to July in Italy, earlier for lower elevations and later for higher areas (*19*). The earlier Mediterranean harvest cases (by mid/late June) render the entire growing season outside the summer BCP growth period, and in the other cases, there is only a very partial overlap at the very end of the Mediterranean growing season. The growth period stated for latewood IrO growth in (*13*) is not accurate. Latewood IrO forms from mid-May through the whole summer and is only complete in early autumn (September/October) with defoliation [(*36*), pages 46 to 51, and (*37*)]. Other oaks in central and northern Europe generally grow from spring (late April/start of May, but starting a little earlier in some areas) through summer to sometime from late August to mid-September (*19*). This places the IrO latewood as representing typically a later average period (July to August), which is not representative of Mediterranean plants that end their growth period by April to June/July. Some spring-sown Mediterranean crops and tree crops are harvested later (June to August) and offer some partial overlap, while grapes have a later growing period and harvest (end of summer to autumn) more parallel with NH trees (*19*). Olives are harvested even later again, in autumn to winter, moving this crop back partly out of kilter by a few months versus NH trees (*19*).

Therefore, at times when the positive Mediterranean growing season offset might be anticipated as possibly relevant, such as a major reversal and plateau in the ^{14}C calibration curve ~1610 to 1530 BCE (*4*), the relevant information likely does not come from BCP or IrO or the current IntCal. Instead, we need information from a Mediterranean source reflecting the typical Mediterranean growing season and the comparison of this against IntCal. Furthermore, this comparison needs to avoid the complication of likely interlaboratory variation. Data from the two areas should be compared via measurements at the same laboratory under the same conditions.

We address this topic here: Are there recurring episodes of differences in contemporary ^{14}C levels that affect the very assumption, and use, of a common high-precision NH calibration curve for the Mediterranean in the past? We investigate by analyzing a multicomponent dataset centered around data series measured for ^{14}C activity at one laboratory, Hd, to control against the issue of interlaboratory variance, following the model established previously (*15*, *19*, *27*, *38*). We analyze a time interval from the mid-second through earlier first millennia BCE. We compare Hd ^{14}C values for known-age German *Quercus* sp. [German oak (GeO)] samples, as core to the existing NH ^{14}C calibration curve in this period (*1*–*4*), with values from near-absolutely dated juniper wood from the archaeological site of Gordion (GOR) in central Anatolia (i.e., the calendar placement of this time series is known within a handful of years; see below) (Fig. 1B) (*15*, *19*, *27*). These tree rings come from a mid-elevation, semiarid, continental setting characterized by cold wet winters and hot dry summers (*28*), where juniper tree ring growth largely ends by and during the summer (*19*). We examine whether there are periods when intra-annual ^{14}C levels in the GOR samples vary appreciably from those in central Europe measured at the same laboratory and whether any offsets occur under climatic conditions similar to those reported in the Jordanian case (*18*). We then consider comparisons of the Hd measurements with other laboratories to assess the accuracy of the Hd ^{14}C estimates. Last, in an effort to characterize reproducibility and the circumstances where a substantive offset is evident, we further consider two other independent time series of ^{14}C dates from other AMS ^{14}C laboratories on tree rings from Italy and Turkey.

RESULTS

Mediterranean ^{14}C offsets

Conventional gas-proportional low-level counted ^{14}C dates have been run at Hd (i) on a series of known age southern German GeO samples for parts of the second and earlier first millennia BCE (*19*, *38*) and most intensively over the interval 3655 to 3431 cal B.P. (calibrated calendar years before the present) (1705 to 1482 BCE) and (ii) on a *Juniperus* sp. chronology from GOR, central Anatolia (table S1) (*15*, *27*). The latter can be near-absolutely dated via ^{14}C "wiggle matching" (*39*) (with instances of dates on the very same tree rings combined as weighted averages), with the midpoint of the first dated tree ring block placed ~3686 cal B.P. (1737 BCE) versus IntCal04 and IntCal98 (Fig. 1B) (*27*) or 1 year earlier against IntCal13. This fit uses all data. In the past, arguments have been made to favor the older part of the chronology due to excessive "noise" in some of the later part of the chronology, and thus, a date placement 10 years later has also been used (*27*). Here, we use the all-data best fit because the noise likely is, in fact, part of the offset issue that we are exploring (*19*). The GOR time

series is compared over its entire extent against the GeO- and IrO-dominated NH ^{14}C calibration records for this period, using the existing IntCal98 and IntCal04 datasets (*1*, *2*) with linear interpolation to 1-year intervals in Fig. 2A. We note that this is different from having original annual measured ^{14}C data; in the absence of these, we have interpolated from ^{14}C measurements on ~5- or ~10-year blocks of wood to estimate 1-year values for the purposes of enabling comparisons between datasets. We compare our data with these two records specifically because they do not include subsequent Hd GeO data (*38*), avoiding circularity. The ^{14}C values from the Hd GOR and GeO records over the interval 3655 to 3431 cal B.P. (1706 to 1482 BCE) are shown compared via linear interpolation to 0.5-year intervals in Fig. 2B. We observe that, in overall net terms, there is reasonable agreement between the records. However, in detail, there are nine recurring substantive positive offset episodes (defined arbitrarily as offsets where in a contiguous period of ≥20 calendar years, ≥95% of those years exhibit a positive offset, i.e., an offset value above 0)—in every instance but one (see below), these correspond with major reversals and plateaus in the ^{14}C record—where the Hd GOR values are consistently older than those from (i) the parallel Hd GeO time series and (ii) the IntCal98 and IntCal04 calibration datasets (table S2). The timing and magnitude of these episodic offsets match the patterns and associations identified 1600 to 1900 CE from Jordan juniper trees (*18*), suggesting a common systemic link over, at least, the past 3700 years. The offsets are typically in the range found previously for substantive seasonal or growing season differences: ~2 to 4‰ (that is, ~16 to 32 ^{14}C years) (*15*–*18*, *23*, *26*). The exception is the offset during the grand solar minimum centered ~750 BCE, which reflects another and less common process (*15*).

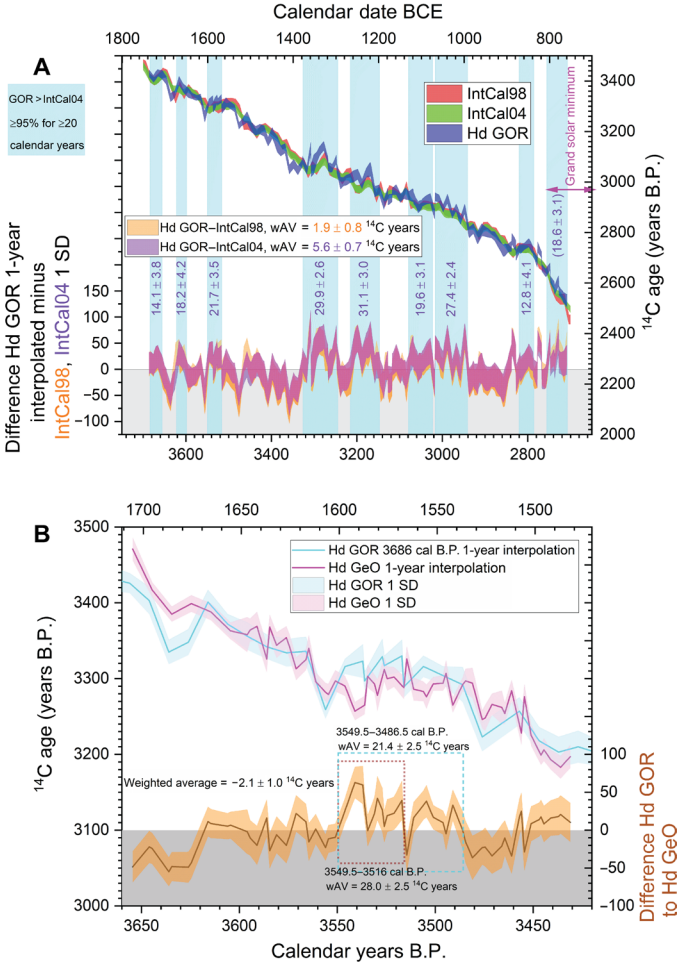

Fig. 2. Comparisons of the 1- or 0.5-year linear interpolated Hd GOR dataset with other NH calibration datasets. (**A**) Comparison of the Hd GOR dataset placed as in Fig. 1B (3686 cal B.P., 1737 BCE) versus the IntCal98 (*1*) and IntCal04 (*2*) calibration curves. Differences (weighted averages) in ^{14}C years are indicated overall and for nine periods where larger positive offsets are apparent for ≥95% of ≥20 consecutive years. (**B**) Comparison of the Hd GOR and Hd GeO time series. The overall difference is shown, and the larger positive offsets apparent 3549.5 to 3516 cal B.P. and 3549.5 to 3486.5 cal B.P. are indicated. All error bands shown are 1 SD.

At the same time, we must also note the reverse observation: At various intervals, particularly where we compare data measured at the same Hd laboratory, there are also some periods of similar scale substantive negative ^{14}C offsets (Fig. 2B). For example, applying the same criteria as above but in reverse, the periods 3654.5 to 3618.5 cal B.P. (1705.5 to 1669.5 BCE) and 3485.5 to 3458.5 cal B.P. (1536.5 to 1509.5 BCE) exhibit negative offsets of (weighted averages) −38.1 ± 2.3 ^{14}C years B.P. and −24.1 ± 3.4 ^{14}C years B.P. These two occurrences correspond with stronger slopes in the ^{14}C calibration curve with declining ^{14}C ages B.P. The comparison with IntCal04 in Fig. 2A would also suggest some other likely sustained negative offsets periods, for example, 3424 to 3400 cal B.P. and 3395 to 3329 cal B.P. (1475 to 1451 BCE and 1446 to 1380 BCE) and 2906 to 2847 cal B.P. (957 to 898 BCE). Again, these are periods where there is a sustained slope in the IntCal record [indicating increased ^{14}C production and, likely, lower solar irradiance (*6*, *15*, *26*)] and steadily declining ^{14}C values. These negative offsets, while not the focus of the present paper, will also be relevant to high-resolution ^{14}C dating in the Mediterranean and hence further undermine the application of a single NH calibration (like IntCal) for the region when seeking high-precision dating.

We carried out two further independent Mediterranean region tests of this situation through examination of time series of ^{14}C dates run at laboratories other than Hd: first, on *Quercus* sp. samples from the Noceto (NOC) site in northern Italy (table S1) (*19*) and, second, on a *Pinus brutia* sample from earlier Iron Age Oymaağaç Höyük (OYM) in north central Turkey (table S1) (*19*). The NOC time series covering the mid-17th through early 15th centuries BCE includes the major and sustained ^{14}C reversal in the earlier 16th century BCE, which is clearly evident in the Hd GOR dataset, especially 3549 to 3517 cal B.P. (1600 to 1568 BCE) and generally 3549 to 3487 cal B.P. (1600 to 1538 BCE) (Fig. 2B). It is worth highlighting that neither the Hd GOR nor the NOC data indicate elevated ^{14}C ages ~3600 to 3555 cal B.P. (1651 to 1606 BCE), contrary to the AA data on BCP and IrO (*13*). The OYM time series lies in the range of a more modest ^{14}C reversal ~2835 to 2795 cal B.P. (~886 to 846 BCE), which, while exhibiting a little noise, is not especially conspicuous in the Hd GOR dataset; the smallest of the offset periods indicated ~2820 to 2785 cal B.P. (~871 to 836 BCE) (Fig. 2A and table S2). As tree ring sequenced sets of ^{14}C data, the series are expected to match the NH calibration curve. However, the NOC time series very clearly does not match IntCal and suggests an offset like the GOR dataset in the earlier 16th century BCE (Fig. 3A), with the three early 16th century BCE NOC values indicating a weighted average offset of 27.4 ± 11.4 ^{14}C years. The OYM time series as a whole, in contrast, indicates noise but does not show any substantive offset (−6.1 ± 6.3 ^{14}C years) and instead offers a spread of ages around the IntCal curve (Fig. 3B). A difference

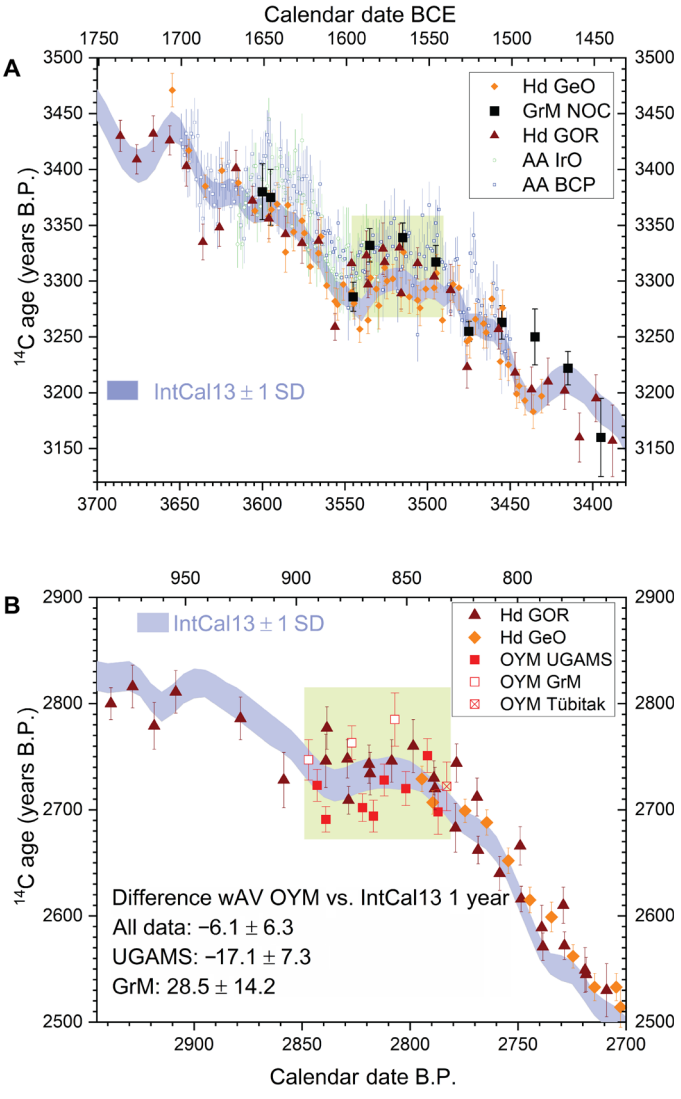

Fig. 3. Comparison of the NOC and OYM data versus Hd GeO, Hd GOR, IntCal13 (1 SD band), and AA BCP and AA IrO (*13*). (**A**) GrM data (weighted averages) on the NOC oak samples (table S1) as best placed (μ ± σ) via a wiggle match (*39*) versus Hd GOR (Fig. 2A). (**B**) The GrM, UGAMS, and Tübitak data on the OYM pine sample (table S1) shown as best placed (μ ± σ) versus IntCal13 (*4*). The shaded areas indicate (A) the earlier 16th century BCE offset in the NOC and Hd GOR data and (B) the mixed GrM and UGAMS signal for OYM versus IntCal13.

between the data from the two laboratories providing measurements is, however, evident. The three Groningen MICADAS (GrM) data do indicate a substantive offset of 28.5 ± 14.2 ^{14}C years, whereas the University of Georgia AMS (UGAMS) data ($n = 8$) rather indicate the reverse with a difference of −17.1 ± 7.3 ^{14}C years. This situation highlights the challenge of interlaboratory variation at high resolution. Nonetheless, the strength of time series wiggle-match dating is revealed, despite such issues, since the UGAMS and GrM sets treated separately find the same most likely placement for the OYM tree rings (mode of probability distributions) within 2 calendar years, which is an inconsequential difference.

The GOR and NOC data indicate the earlier 16th century BCE as a Mediterranean positive offset instance of the type and scale of those observed in the Jordan cases in the second millennium CE (*18*), notably for both the central Mediterranean (NOC) and the east Mediterranean (GOR), demonstrating wider area relevance, but the negative (or unclear) OYM case demonstrates that such a clear, substantive offset does not necessarily occur in every case and perhaps not in cases of more minor ^{14}C reversals [the 2820 to 2785 cal B.P. (871 to 836 BCE) interval indicated in Fig. 2A partly overlaps the OYM series, but it is the smallest of the offset intervals noted (13.2 ± 3.5 ^{14}C years) for the Hd GOR time series]. This suggests that there may be an effect threshold and that, perhaps, additional factors associated with at least some major and sustained ^{14}C reversals must also come into play to create the observed substantive ^{14}C offset episodes. Hence, positive identification of other offset intervals will require further direct work and data. In the interim, the GOR and NOC data confirm the potential relevance and scale of a temporally fluctuating Mediterranean offset (*18*) over the longer term and as relevant to prehistoric dating at high resolution in the Mediterranean region (Figs. 2A and 3A). For the Mediterranean, this means that ^{14}C calibration curves constructed from data from midlatitude NH trees, such as IntCal (*4*), are potentially less appropriate, especially during periods of major and sustained ^{14}C reversals.

Interlaboratory ^{14}C differences

The Hd GeO versus GOR comparison in the earlier 16th century BCE highlights a difference, a ^{14}C offset, that is independent of variations in absolute values achieved by different laboratories. There is a long history of even the most accurate ^{14}C laboratories systematically varying in age determinations for contemporary samples compared with other laboratories by up to ~30 ^{14}C years (*1*, *2*). Recent work measuring known-age high-elevation BCP tree rings (whole ring) from North America and late-wood from low-elevation IrO over the common period 3615 to 3529 cal B.P. (1666 to 1580 BCE) achieved relatively similar results for both datasets (BCP older by 6.4 ± 2.0 ^{14}C years, weighted average) (*13*) but found values varying by ~20 to 40 ^{14}C years versus previous measurements on German and Irish tree rings in IntCal for the 17th to 16th centuries BCE (*13*). What we have identified instead, comparing Hd GeO and Hd GOR, is a systematic difference, or offset, based on the source of wood (and thence growing season) and not the laboratory. Thus, even when subsequent iterations of IntCal (such as the forthcoming IntCal20) are modified to reflect additional data input [such as those data in (*13*)], this apparent difference of Mediterranean wood versus central European wood in the earlier 16th century BCE observed within the Hd datasets remains real and relevant.

As discussed above, neither the BCP nor latewood IrO is a good representation of the main lower-elevation Mediterranean growing season. Instead, the BCP and the IrO should offer a dataset similar to those reflecting central and northern European later spring-summer growing seasons, such as the GeO and IrO comprising much of the existing IntCal dataset in this time period, despite a history of issues with BCP ^{14}C data in earlier work (*2*, *14*, *25*). We would therefore have anticipated that the AA data on BCP and IrO (*13*) should be similar to the IntCal datasets (*1*–*4*) and the Hd GeO data (*38*), given the good agreement in other recent work between GeO and BCP (*40*–*42*) and between GeO and IrO (*1*–*4*). However, despite sometimes marked interannual variation, the AA AMS ^{14}C data are, as noted above, typically ~20 to 40 ^{14}C years older than IntCal13 during the period ~1660 to 1540 BCE (Fig. 3A) (*13*). Therefore, this is a laboratory or method difference. If correct, then these AA values on BCP and IrO would, in fact, imply even older ^{14}C ages for the positively

offset GOR samples across this period (Fig. 2B) if they were measured at AA (see below).

The AA findings and other recent work raise concerns over the comparability of low-level gas proportional counting (LLGPC) measurements (e.g., Hd), the basis of most of the existing NH IntCal curve in this period (*1*–*4*), versus some AMS ^{14}C data at high precision (see also fig. S1) (*10*, *12*, *13*) and, thus, in the present context, the correct absolute ^{14}C values for IntCal in the period ~1660 to 1540 BCE. In most work to date, no general pattern of offsets between AMS ^{14}C measurements and LLGPC ^{14}C measurements at Hd is apparent (*19*, *43*–*45*), and many AMS ^{14}C measurement series do not exhibit such an unexpected older offset versus comparable samples measured by LLGPC (*4*, *40*–*42*). A study of the dating of Younger Dryas age wood offers two comparisons (*43*). In the first case, the Hd data were slightly the youngest on average but within 12 to 26 ^{14}C years of the three AMS ^{14}C laboratories and 11 ^{14}C years of the liquid scintillation counting (LSC) laboratory, with all values overlapping substantially within respective population SEs (and, in fact, ~33% of the Hd offset is attributable to one outlying date: for mid-ring 376.5). In the second case, the Hd data were, on average, 21 ^{14}C years younger than the LSC laboratory (Waikato), leading the authors to suggest there was likely a small ~10 to 20 ^{14}C year systematic offset between Hd and Waikato. For the time range of this study, Hd GeO values compare well with previous Seattle LLGPC measurements on GeO 1700 to 1500 BCE (*15*), Oxford (OxA) AMS ^{14}C measurements on GeO 1354 to 1303 BCE (*24*) and on Anatolian juniper from the late 21st to 20th centuries BCE (figs. S2 and S3) (*46*), and Keck Carbon Cycle Accelerator Mass Spectrometry Laboratory, University of California, Irvine AMS ^{14}C measurements on BCP 795 to 625 BCE (fig. S4) (*40*). In the latter three cases, the AMS ^{14}C values are, on average, more recent than the Hd LLGPC ages [contrary to the findings in the comparison in (*43*)]. A comparison of AMS ^{14}C measurements (*47*) versus Hd measurements (table S1) on similar Swedish pine samples also indicates no substantial difference for the 15th to 17th centuries CE (fig. S5). A comparison of AMS ^{14}C dates on single-year known-age wood samples from U.K. contexts in the period of the LLGPC annual ^{14}C dataset from the Seattle laboratory (QL) (*1*) found differences of OxA AMS ^{14}C to QL of only 1.4 ± 7.9 ^{14}C years (n = 25), a difference of Scottish Universities Environmental Research Centre Radiocarbon Dating Laboratory AMS ^{14}C data to QL of 12.1 ± 8.0 ^{14}C years (n = 26), and a difference for Groningen to QL of −22.5 ± 13.6 (n = 6) (*48*). This comparison suggests potentially no offset (OxA) and otherwise small laboratory-specific offsets but in both directions and, thus, no general pattern. Our data indicate a similar mixed picture. In accord with some finds of on average slightly older ^{14}C ages from AMS ^{14}C measurements (*10*, *12*, *13*), we observe that our GrM NOC and GrM OYM Mediterranean AMS ^{14}C data are, respectively, 21.1 ± 8.0 and 28.6 ± 14.4 ^{14}C years older than the corresponding interpolated Hd GOR Mediterranean ages. However, in contrast, the UGAMS OYM AMS ^{14}C dates exhibit an opposite shift of −26 ± 7.7 ^{14}C years to more recent ages. This suggests that interlaboratory variation is also relevant and likely a dominant issue.

Other Mediterranean region data can offer some control on the scale of the possible AMS versus LLGPC issue. An OxA AMS ^{14}C study comparing 18th to 19th century CE annual plant material from Egypt versus the LLGPC NH calibration curve (unstated, but IntCal04/09) obtained an average offset of 19 ± 5 ^{14}C years (*16*), and a comparison of the large New Kingdom (mid-second to early first millennia BCE) AMS ^{14}C dataset of Egyptian samples also found an offset (using the OxCal ΔR function, with a neutral prior of 0,10, which quantifies the possible systematic offset of a set of ^{14}C data versus the reference curve with a normally distributed likelihood) with a mean of ~18 ^{14}C years (generalized as ~20 ± 5 ^{14}C years in the text of ref. (*23*) ; we use this SD below) against LLGPC IntCal04 [(*23*) at fig. 3] [we note that in five reruns of this model against IntCal04, we achieved ΔR test 0,10 μ ± σ results of 15.0 ± 10.4 to 17.8 ± 4.8 ^{14}C years and that using the information added in the table S1 addendum to (*23*), we achieved lower values for a ΔR test 0,10 across five runs of μ ± σ: 11.3 ± 5.4 to 12.0 ± 5.9 ^{14}C years]. A tree-ring time series comprising seven weighted average OxA AMS ^{14}C dates on an oak sample from Miletus in low-elevation western Anatolia offers a close fit to the LLGPC-source IntCal curve (*27*), with an OxCal ΔR 0,10 value versus IntCal09 (μ ± σ) of only 4.0 ± 8.3 ^{14}C years. In each of these cases, this offset includes the Mediterranean offset. If we maintain the same LLGPC IntCal04/09 reference value [the recent tree ring part of the two calibration curves was the same (*2*, *3*)] and an OxCal ΔR 0,10 test, then the OxA and AA Jordan juniper AMS ^{14}C offsets (*18*) are (μ ± σ) 18.2 ± 2.8 and 18.1 ± 4.1 ^{14}C years, respectively. All these values are noticeably in a very similar range. They include both any average AMS to LLGPC difference and the average Mediterranean offset. The equivalent comparison of the LLGPC Hd GOR series versus the LLGPC IntCal04 dataset yields an OxCal ΔR value of 9.2 ± 2.5 ^{14}C years. This offset includes only the Mediterranean offset since it is an LLGPC versus LLGPC comparison. Therefore, this comparison leaves the possibly relevant remaining AMS ^{14}C–to–LLGPC difference as (in order of comparisons above) 9.8 ± 5.6, 8.8 ± 5.6 (5.8 ± 10.7 to 8.6 ± 5.4 or 2.1 ± 6.0 to 2.8 ± 6.7), −5.2 ± 8.7, 9.0 ± 3.8, and 8.9 ± 4.8 ^{14}C years. We could reasonably generalize all this information as ≤10 ^{14}C years. We consider the relevance of this issue below.

DISCUSSION

Egyptian history and ^{14}C offsets

Our findings identify and highlight the relevance of a recurring variable growing season positive ^{14}C offset for the lower-elevation Mediterranean. This recurring phenomenon, with offset episodes variously from ~13 to 31 ^{14}C years (Fig. 2A), undermines the relevance of the generic midlatitude NH ^{14}C calibration curve for high-resolution chronology in the Mediterranean and especially during these offset episodes. As an example, we may highlight and confirm the relevance of these periods of difference by comparing the time series of ^{14}C data from the historically sequenced New Kingdom Egypt dataset (*23*) placed against IntCal04 versus the Hd GOR ^{14}C record from Fig. 2A, as shown in Fig. 4A. There are several periods where the ^{14}C dates on the Egyptian samples, in fact, appear to fit the pattern of the Mediterranean-relevant Hd GOR record much better than the IntCal04 (*2*) record, as well as without application of a static correction factor (*16*, *23*). The dates for samples from the tomb of Tutankhamun at Thebes offer a good test case (*23*, *24*). Mainstream assessments of historical sources place the time range for the accession of Tutankhamun (the king and his court subsequently leave Amarna for Memphis early in his reign) and his death likely in his 9th or 10th year, somewhere between ~1336/1325 and 1327/1316 BCE (*23*, *24*, *49*). The coherent weighted average ^{14}C date from a set of samples (using six of seven available dates) from the funerary context of Tutankhamun is 3117 ± 12 ^{14}C years B.P. If we compare the intersection of these calendar and ^{14}C ranges, we see a better fit with the Hd GOR calibration range (Fig. 4A). The placement of the Tutankhamun data set rerunning the analysis in (*24*) against

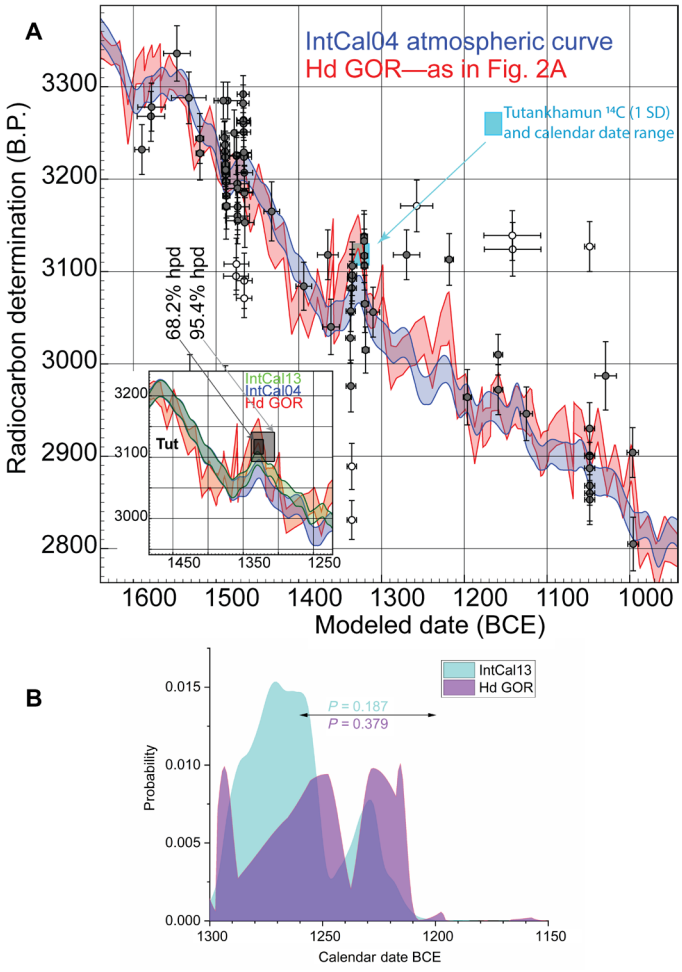

Fig. 4. Two example chronological ramifications from the Mediterranean ^{14}C record and offsets indicated by the Hd GOR dataset. (**A**) Egyptian date series as reported and placed against IntCal04 (*23*) compared with Hd GOR curve from Fig. 2A (curves are shown as 1 SD bands, and data were plotted as 1 SD ranges of ^{14}C ages and modeled calendar age ranges). Data that are almost certain to be outliers (*23*) have white center points. Cyan box indicates weighted average ^{14}C (1 SD) and calendar range for Tutankhamun (Tut). Inset: Modeled placement 68.2 and 95.4% highest posterior density (hpd) of Tut against IntCal13 (*4*) from the OxCal model in (*24*) and compared with IntCal04 (*2*) and Hd GOR (Fig. 2A). (**B**) The difference in 13th century BCE dating probability comparing the calendar age probabilities for 3035 ± 15 ^{14}C years B.P. from the Hd GOR data (Fig. 2A) versus IntCal13 calibration curve (*4*). Data from OxCal (*59*) with curve resolution set to 1 year.

IntCal13 and comparing against IntCal04 and Hd GOR similarly shows a likely best fit versus the Hd GOR range (Fig. 4A, inset).

Eight apparent offset intervals for attention

Within our study, eight periods are noted where substantive offsets likely associated with a typical Mediterranean growing season are evident. These periods for further attention are indicated in Fig. 2A and table S2 [the grand solar minimum period 750 ± 60 BCE (*50*) likely reflects a different process (*15*)]. Some of these periods of reversals and plateaus in the atmospheric ^{14}C record are moreover likely associated with climate change episodes since marked changes in ^{14}C production and availability in the troposphere in the Holocene reflect changes in solar activity and ocean systems (*51*, *52*) and, thus, may sometimes be associated with periods of cultural transition. For example, the time intervals around the termination of the Late Bronze Age (mid–later 13th century BCE) and during the earlier Iron Age (11th century BCE) stand out as two culturally important time intervals when major transformations or reorientations in historical trajectories are often linked with climate perturbations (*19*, *52*, *53*). These transitions are coeval with periods in the GOR record that are offset from the IntCal records (Fig. 2A), and hence, small but potentially important revisions to chronology might be suspected and will be crucial to defining and interpreting historical narratives (*18*, *19*, *53*). We give a specific example and illustration of how the calendar time range to be associated with a given ^{14}C date can change. A hypothetical ^{14}C date of 3035 ± 15 ^{14}C years B.P. has double the calendar probability (37.9% versus 18.7%) for the critical date range between 1260 and 1200 BCE when contrasting the Hd GOR versus IntCal13 ^{14}C calibration datasets (Fig. 4B).

Thera/Santorini eruption date

The earlier 16th century BCE Mediterranean offset identified above in the Hd GOR and GrM NOC datasets is particularly relevant to a long-running controversy: the dating of the Minoan eruption of the Thera (Santorini) volcano and associated debates around its impacts and the chronology of the beginning of the Aegean Late Bronze Age (*13*, *19*, *54*–*58*). Scholarship until now has used the various versions of the NH IntCal ^{14}C calibration curve. Although the 16th century BCE reversal in the calibration curve has long been noted as potentially creating a dating ambiguity for the Thera eruption between the later 17th century BCE and the earlier mid–16th century BCE, the weight of probability has supported the older age range in the later 17th century BCE and, thus, a date over 100 year earlier than the pre-radiocarbon archaeological estimates ~1500 BCE (*57*). A recent contribution, seeking a compromise, is a proposal to revise the IntCal ^{14}C calibration curve ~1660 to 1540 BCE based on measurements of BCP and IrO at AA, which yield older ^{14}C ages for this interval than IntCal13 (*13*). However, the identification of a specific Mediterranean offset in the earlier 16th century BCE (Figs. 2, A and B, and 3A) indicates that the correct date will not solely derive from IntCal nor do these BCP and IrO samples reflect the typical Mediterranean growing season (see above). There is instead a specific Mediterranean context for this controversy. Thus, rather than (or in addition to) adjusting the overall IntCal calibration curve (important although this is, in general, when justified), instead, it is the effect of the Mediterranean offset at this period that is relevant. In particular, as evident in Figs. 2 (A and B) and 3A, the Hd GOR and GrM NOC data indicate that Mediterranean ^{14}C ages in the earlier 16th century BCE are older than the IntCal values and, thus, are potentially approximately contemporary with ^{14}C ages for the last decades of the 17th century BCE. This could exacerbate the dating ambiguity between the later 17th century BCE and the earlier mid–16th century BCE. At the same time, the absence of elevated ^{14}C ages for the Mediterranean Hd GOR and NOC samples ~3600 to 3555 cal B.P., contrary to the AA BCP and IrO dataset (Fig. 3A) (*13*), is also important for this topic.

We can assess the implications and remaining uncertainties. The calibrated calendar probabilities for dating the Santorini eruption following two published methods (*55*, *56*) can be compared with the Hd GOR scenario. If we rerun these analyses with the Hd GOR calibration dataset (as in Fig. 2A) with its revision of the earlier mid–16th century BCE ^{14}C values to reflect Mediterranean conditions and regional offset, we find that the results support a later 17th century

BCE date range for the Thera eruption, including the entire most likely 68.2% highest posterior density (hpd) ranges (Fig. 5, A and B; 1649 to 1617 BCE and 1680 to 1613 BCE, respectively). We may also reconsider the dating of the Thera olive branch sample, found buried in the Thera eruption pumice (*58*), modeled as an ordered sequence of older to more recent wood to obtain a dating estimate for the outermost dated sample (*13*, *54*) against the Hd GOR dataset (Fig. 5C). This places all the 68.2% hpd range in the 17th century BCE and most (76.6% versus 18.7%) of the 95.4% hpd range at or before 1610 BCE and hence again likely indicates a later 17th century BCE date range. Thus, the Mediterranean-relevant Hd GOR dataset does not indicate the ambiguous 17th or 16th century calibrated ranges for the Thera eruption proposed in (*13*) from the AA BCP and IrO data. In the case of the olive branch, we may note one additional important element: The dates on the sample were run as LLGPC measurements at the Hd ^{14}C laboratory (*58*). Hence, there is no possible AMS ^{14}C–to–LLGPC issue in this case. Instead, we have comparable Mediterranean Hd measurements against Mediterranean Hd measurements. The finding is most likely a later 17th century BCE date range for this sample (*19*).

The remaining caveat is the issue of whether there is, in addition, a typical AMS ^{14}C–to–LLGPC offset that we should take into account when considering AMS ^{14}C dates. As discussed above, the evidence is mixed. Nonetheless, consideration above of some Mediterranean AMS ^{14}C cases suggested that perhaps an additional factor of ≤10 ^{14}C years might apply to the LLGPC Hd GOR dataset versus AMS ^{14}C dates. These comparisons especially including OxA AMS ^{14}C data are particularly relevant to the Thera case since OxA AMS ^{14}C data, or the demonstrated very comparable Vienna (VERA) AMS ^{14}C data (*23*, *46*, *55*), comprise 79% and 75% of the two datasets (*55*, *56*) for the Thera volcanic destruction level. If we rerun the analyses in Fig. 5 (A and B) with an additional hypothetical +10 ^{14}C years adjustment to the Hd GOR dataset, then we do not find a substantial change (Fig. 5, D and E). The dating probabilities still continue to indicate the later 17th century BCE as the most likely date range. To effect substantive change, a putative AMS to LLGPC offset would need to be rather larger. If it were to reach around 15 ^{14}C years, then the date of the Santorini eruption starts to become more ambiguous. There is still greater probability in the later 17th century BCE, but moderate probability now lies in the earlier mid–16th century BCE (Fig. 5, F and G). Only if the hypothetical adjustment is 20 or 25 ^{14}C years, does the dating probability switch to indicating that an earlier mid–16th century BCE date range is more likely (Fig. 5, H to K). However, despite some data suggesting larger AMS ^{14}C–to–LLGPC differences of around this level (*10*, *12*, *13*), the Mediterranean cases reviewed above only suggest a difference of about half this level (or less), other comparisons are mixed, and some are even close to zero (see above). Much of the current observed variation is as likely to relate to interlaboratory variations in methods and instruments [an ever-present issue (*8*, *11*, *48*)], something only more evident as AMS ^{14}C approaches the precision of LLGPC and LSC datasets. The conclusion at present is that more work is needed to clarify and quantify the status of any typical AMS ^{14}C–to–LLGPC ^{14}C offset on comparable samples, that is, an offset that is common across multiple AMS ^{14}C laboratories and not cases of individual interlaboratory variations (up and down) within an overall range of values. In the case of the Thera olive branch sample, this avoids any possible AMS ^{14}C–to–LLGPC issue since it was measured at Hd using LLGPC (*58*). Here, comparison with the Mediterranean relevant Hd GOR dataset indicates a most likely later 17th century BCE date range

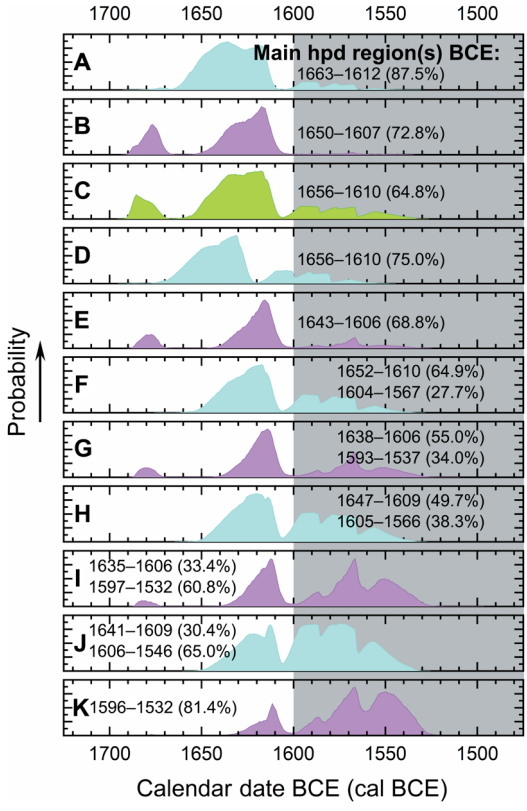

Fig. 5. Calendar dating probability estimates for the Santorini/Thera volcanic destruction level from the data and models in (*55*) (cyan) and (*56*) (magenta) and the olive branch outer dated segment (*13*, *54*, *58*) (green) given changing calibration scenarios (*39*, *59*). (**A** to **C**) With Hd GOR calibration dataset in Fig. 2A. (**D** and **E**) Application of a hypothetical addition of +10 ^{14}C years to Hd GOR to reflect a putative AMS ^{14}C offset to LLGPC measurements. (**F** and **G**) Application of a hypothetical +15 ^{14}C years. (**H** and **I**) Application of a hypothetical +20 ^{14}C years. (**J** and **K**) Application a hypothetical +25 ^{14}C years. Main hpd regions are those contiguous intervals identified within the overall 95.4% hpd ranges.

(Fig. 5C), which is consistent with the analysis of sets of AMS ^{14}C data against the Hd GOR dataset (Fig. 5, A and B). This suggests the reality of an additional AMS ^{14}C–to–LLGPC contribution of no more than about ≤10 ^{14}C years, as discussed above.

The situation could change if future work can, to the contrary, robustly demonstrate a much larger standard AMS ^{14}C–to–LLGPC offset. We also need to better define (and enlarge the database concerning) the Mediterranean offset independent of these questions of interlaboratory and intermethod variations. Already, we can likely set the parameters of the extreme alternative scenario with respect to the Santorini eruption case using the available data and the same models (*13*, *54*–*56*, *58*). The BCP record of (*13*) likely exhibits a maximum alternative case for a revised AMS ^{14}C IntCal summer NH baseline (Fig. 6, A to C) (*19*). We can then, in addition, consider the possible relevance of the positive average offset of ~21 ^{14}C years between the Mediterranean and NH in the period ~3550 to 3486 cal B.P. (1601 to 1537 BCE) as identified from the comparison of the Hd datasets (Fig. 2B) and apply this adjustment to the AA BCP data (Fig. 6, D to F). In this hypothetical experiment, we treat the remainder of the period ~3600 to 3450 cal B.P. (1651 to 1501 BCE) as not being substantively offset (Figs. 2B and 3A). The probability distributions

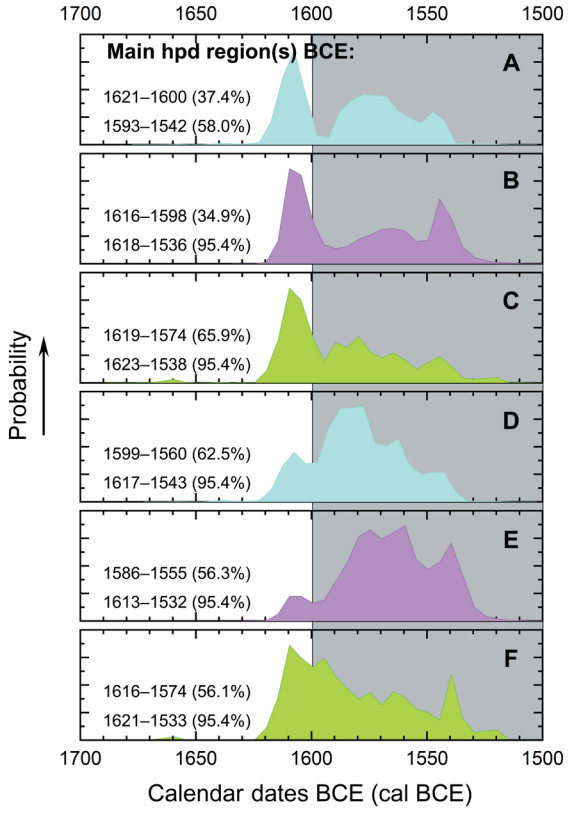

Fig. 6. Hypothetical calendar dating probability estimates for the Santorini/Thera volcanic destruction level from the data and models in (*55*) (cyan) and (*56*) (magenta) and the olive branch outer dated segment (*13*, *54*, *58*) (green) using a likely maximum possible change scenario. (**A** to **C**) With AA BCP calibration dataset (*13*) with a curve resolution of 5 years (smoothing the noisy 1-year data). (**D** to **F**) Application of a hypothetical further addition of +21 ^{14}C years ~3550 to 3486 cal B.P. (1601 to 1537 BCE) to reflect the positive Mediterranean offset (Fig. 2B); curve resolution, 5 years (smoothing the noisy 1-year data). Main hpd regions are those contiguous intervals identified within the overall 68.2 and 95.4% hpd ranges.

in Fig. 6 illustrate the extreme alternative dating scenarios. The published AA BCP record (Fig. 6, A to C) creates an ambiguous situation: A clear probability region remains in the late 17th century BCE to early 16th century BCE, but there is also considerable probability in the mid–16th century BCE. However, were the approximate range of the AA BCP data to form a new IntCal baseline and a Mediterranean positive offset to also apply in addition (a logical implication, but needing empirical testing), then the dating probability starts more strongly to support an early to mid–16th century BCE date. Such a scenario [or the hypothetical large LLGPC to AMS ^{14}C adjustments considered in Fig. 5 (H to K)], interestingly, does not, however, return us to the traditional "low" archaeological chronology (*19*, *57*). Instead, it would point to a possible alternative between the current "high" and low scenarios: a shortened "compromise early chronology" for the date of the Santorini eruption and the earlier Aegean Late Bronze Age (*19*, *56*). Even at the extreme hypothetical adjustment range (Figs. 5, H to K, and 6, A to F), the traditional date range of the Santorini eruption ~1500 BCE (*57*), or any date after ~1530 BCE, appears highly improbable.

Overall, our findings, both the periods of positive ^{14}C offsets that we focus on in this paper, as well as the instances of periods of negative offsets noted above, in addition to other indications of similar Mediterranean or seasonal ^{14}C offsets (*8*, *14*–*19*), highlight the relevance of these recurring offset elements to high-resolution absolute dating for Old World prehistory. This topic assumes greater and greater importance as ^{14}C dating and chronometric aspirations become ever more accurate and precise. We may draw two key conclusions. First, there is now clearly a need going forward for the development of a detailed consensus Mediterranean ^{14}C time series to secure an appropriate closely defined Old World archaeological time scale. No simple static adjustment is possible as a satisfactory solution for the recurring, periodic offsets observed in both the BCE and CE windows reported in works to date. Second, it is necessary to establish greater temporal and spatial delineation of seasonal/growing season variations for accurate high-precision ^{14}C dating worldwide.

MATERIALS AND METHODS

Experimental design

The main aim of this study is to compare time series of radiocarbon (^{14}C) measurements on tree ring samples and, in particular, to compare data from trees with typical lower-elevation Mediterranean growth contexts versus those from central and northern Europe, which comprise most of the midlatitude NH international radiocarbon calibration curve [IntCal, through different iterations (*1*–*4*)]. We sought to investigate whether a likely growing season–related offset occurred periodically in the past, as has been reported in a more recent period (*18*). In particular, a key aim of the study is to compare data from a central European time series (GeO from southern Germany) versus data from a Mediterranean time series (*Juniperus* sp. from central Anatolia), which were measured in the same laboratory (the LLGPC facility at Hd) under the same conditions. This parallel dating strategy circumvents the problem of being unable, otherwise, to extract signal from the noise of interlaboratory variation, which is often the cause for any apparent differences. Thus, regardless of the absolute dating accuracy of the Hd laboratory over this period, the relative similarities or differences observed between the two Hd time series are real. We then tested one period where a difference in values was observed with an additional series of measurements on wood from Italy at another laboratory using a different method (AMS ^{14}C), and we investigated and compared another period where a more modest difference was observed with wood from northern Anatolia using data from three AMS ^{14}C laboratories. For details on the laboratory procedures at each ^{14}C laboratory and the tree ring samples used, see the Supplementary Materials (*19*). We note that three ^{14}C measurements were excluded as unexplained too old outliers and remeasurements of these samples are used instead (see table S1).

The tree ring series wiggle matches (*39*) and calibrated calendar dating probabilities shown in Figs. 2 to 5 were obtained using the OxCal software (*59*). OxCal version 4.3.2 was used, except for the analysis in Fig. 4A, which used version 4.1.7 as did the reruns of the model in (*23*) mentioned in the main text (Results). Curve resolution of 1 year was used. For discussion and information about the use of OxCal and the specific outlier models and coding, see the Supplementary Materials (*19*).

Statistical analysis

Radiocarbon calibration and wiggle matching used the OxCal software (*19*, *59*) as noted. Interpolation of ^{14}C time series to 1-year increments used linear extrapolation. Where 10-year tree ring blocks

are involved, the midpoint is treated as year 5.5 of the series, and 0.5-year increments were interpolated as necessary. In cases of ^{14}C dates run on the identical (same age) tree ring years, these were combined into weighted averages and errors (*19*). Differences between ^{14}C time series were calculated from the set of paired comparisons (either corresponding 1- or 0.5-year interpolated intervals or paired data) and their combined (propagated) errors.

SUPPLEMENTARY MATERIALS

Supplementary material for this article is available at http://advances.sciencemag.org/cgi/content/full/6/12/eaaz1096/DC1

Supplementary Materials and Methods

Fig. S1. Comparisons of some ETH AMS ^{14}C data on known-age Mediterranean samples versus Hd data and IntCal98 and IntCal04/09.

Fig. S2. Comparison of Hd GeO LLGPC measurements (*38*) with OxA AMS ^{14}C measurements on similar GeO (*24*).

Fig. S3. Comparison of the OxA AMS ^{14}C measurements versus Hd LLGPC measurements on Anatolian juniper samples from a Middle Bronze Age dendrochronological time series built from *Juniperus* sp. samples from the archaeological sites of Kültepe, Acemhöyük, and Karahöyük (*46*).

Fig. S4. Comparison of Keck Carbon Cycle Accelerator Mass Spectrometry Laboratory, University of California, Irvine AMS ^{14}C dates on known-age BCP (*40*) versus similar known-age GeO Hd LLGPC ^{14}C data (*38*).

Fig. S5. Comparison of AMS ^{14}C data versus Hd LLGPC ^{14}C ages for similar Swedish pine.

Fig. S6. Cross-dating grid for the NOC *Quercus* sp. chronology.

Fig. S7. The indexed tree ring series comprising the NOC *Quercus* sp. chronology.

Fig. S8. The tree ring measurements of the NOC-12 and NOC-14 samples within the NOC chronology.

Table S1. ^{14}C data used in this paper for Figs. 1 to 3 and figs. S1 and S5.

Table S2. The nine offset periods identified in Fig. 2A.

References (*60*–*152*)

REFERENCES AND NOTES

1. M. Stuiver, P. J. Reimer, T. F. Braziunas, High-precision radiocarbon age calibration for terrestrial and marine samples. *Radiocarbon* **40**, 1127–1151 (1998).
2. P. J. Reimer, M. G. L. Baillie, E. Bard, A. Bayliss, J. W. Beck, C. J. H. Bertrand, P. G. Blackwell, C. E. Buck, G. S. Burr, K. B. Cutler, P. E. Damon, R. L. Edwards, R. G. Fairbanks, M. Friedrich, T. P. Guilderson, A. G. Hogg, K. A. Hughen, B. Kromer, G. M. Cormac, S. Manning, C. B. Ramsey, R. W. Reimer, S. Remmele, J. R. Southon, M. Stuiver, S. Talamo, F. W. Taylor, J. van der Plicht, C. E. Weyhenmeyer, IntCal$_{04}$ terrestrial radiocarbon age calibration, 0–26 cal kyr BP. *Radiocarbon* **46**, 1029–1058 (2004).
3. P. J. Reimer, M. G. L. Baillie, E. Bard, A. Bayliss, J. W. Beck, P. G. Blackwell, C. Bronk Ramsey, C. E. Buck, G. S. Burr, R. L. Edwards, M. Friedrich, P. M. Grootes, T. P. Guilderson, I. Hajdas, T. J. Heaton, A. G. Hogg, K. A. Hughen, K. F. Kaiser, B. Kromer, F. G. McCormac, S. W. Manning, R. W. Reimer, D. A. Richards, J. R. Southon, S. Talamo, C. S. M. Turney, J. van der Plicht, C. E. Weyhenmeyer, IntCal09 and Marine09 radiocarbon age calibration curves, 0–50,000 years Cal BP. *Radiocarbon* **51**, 1111–1150 (2009).
4. P. J. Reimer, M. G. L. Baillie, E. Bard, A. Bayliss, J. W. Beck, P. G. Blackwell, C. B. Ramsey, C. E. Buck, H. Cheng, R. L. Edwards, M. Friedrich, P. M. Grootes, T. P. Guilderson, H. Haflidason, I. Hajdas, C. Hatté, T. J. Heaton, D. L. Hoffmann, A. G. Hogg, K. A. Hughen, K. F. Kaiser, B. Kromer, S. W. Manning, M. Niu, R. W. Reimer, D. A. Richards, E. M. Scott, J. R. Southon, R. A. Staff, C. S. M. Turney, J. van der Plicht, IntCal13 and Marine13 radiocarbon age calibration curves 0–50,000 years Cal BP. *Radiocarbon* **55**, 1869–1887 (2013).
5. T. F. Braziunas, I. Y. Fung, M. Stuiver, The preindustrial atmospheric $^{14}CO_2$ latitudinal gradient as related to exchanges among atmospheric, oceanic, and terrestrial reservoirs. *Global Biogeochem. Cycles* **9**, 565–584 (1995).
6. M. Stuiver, T. F. Braziunas, Anthropogenic and solar components of hemispheric ^{14}C. *Geophys. Res. Lett.* **25**, 329–332 (1998).
7. Q. Hua, M. Barbetti, A. R. Rakowski, Atmospheric radiocarbon for the period 1950–2010. *Radiocarbon* **55**, 2059–2072 (2013).
8. U. Büntgen, L. Wacker, J. D. Galván, S. Arnold, D. Arseneault, M. Baillie, J. Beer, M. Bernabei, N. Bleicher, G. Boswijk, A. Bräuning, M. Carrer, F. C. Ljungqvist, P. Cherubini, M. Christl, D. A. Christie, P. W. Clark, E. R. Cook, R. D'Arrigo, N. Davi, Ó. Eggertsson, J. Esper, A. M. Fowler, Z.'. Gedalof, F. Gennaretti, J. Grießinger, H. Grissino-Mayer, H. Grudd, B. E. Gunnarson, R. Hantemirov, F. Herzig, A. Hessl, K. U. Heussner, A. J. T. Jull, V. Kukarskih, A. Kirdyanov, T. Kolář, P. J. Krusic, T. Kyncl, A. Lara, C. LeQuesne, H. W. Linderholm, N. J. Loader, B. Luckman, F. Miyake, V. S. Myglan, K. Nicolussi, C. Oppenheimer, J. Palmer, I. Panyushkina, N. Pederson, M. Rybníček, F. H. Schweingruber, A. Seim, M. Sigl, O. Churakova, J. H. Speer, H. A. Synal, W. Tegel, K. Treydte, R. Villalba, G. Wiles, R. Wilson, L. J. Winship, J. Wunder, B. Yang, G. H. F. Young, Tree rings reveal globally coherent signature of cosmogenic radiocarbon events in 774 and 993 CE. *Nat. Commun.* **9**, 3605 (2018).
9. J. Uusitalo, L. Arppe, T. Hackman, S. Helama, G. Kovaltsov, K. Mielikäinen, H. Mäkinen, P. Nöjd, V. Palonen, I. Usoskin, M. Oinonen, Solar superstorm of AD 774 recorded subannually by Arctic tree rings. *Nat. Commun.* **9**, 3495 (2018).
10. R. Friedrich, B. Kromer, F. Sirocko, J. Esper, S. Lindauer, D. Nievergelt, K. U. Heussner, T. Westphal, Annual ^{14}C tree-ring data around 400 AD: Mid- and high-latitude records. *Radiocarbon* **61**, 1305–1316 (2019).
11. E. M. Scott, G. T. Cook, P. Naysmith, R. A. Staff, Learning from the wood samples in ICS, TIRI, FIRI, VIRI, and SIRI. *Radiocarbon* **61**, 1293–1304 (2019).
12. D. Güttler, L. Wacker, B. Kromer, M. Friedrich, H.-A. Synal, Evidence of 11-year solar cycles in tree rings from 1010 to 1110 AD—Progress on high precision AMS measurements. *Nucl. Instrum. Meth. B* **294**, 459–463 (2013).
13. C. L. Pearson, P. W. Brewer, D. Brown, T. J. Heaton, G. W. L. Hodgins, A. J. T. Jull, T. Lange, M. W. Salzer, Annual radiocarbon record indicates 16th century BCE date for the Thera eruption. *Sci. Adv.* **4**, eaar8241 (2018).
14. F. G. McCormac, M. G. L. Baillie, J. R. Pilcher, R. M. Kalin, Location-dependent differences in the ^{14}C content of wood. *Radiocarbon* **37**, 395–407 (1995).
15. B. Kromer, S. W. Manning, P. I. Kuniholm, M. W. Newton, M. Spurk, I. Levin, Regional $^{14}CO_2$ offsets in the troposphere: Magnitude, mechanisms, and consequences. *Science* **294**, 2529–2532 (2001).
16. M. W. Dee, F. Brock, S. A. Harris, C. B. Ramsey, A. J. Shortland, T. F. G. Higham, J. M. Rowland, Investigating the likelihood of a reservoir offset in the radiocarbon record for ancient Egypt. *J. Archaeol. Sci.* **37**, 687–693 (2010).
17. S. W. Manning, M. W. Dee, E. M. Wild, C. Bronk Ramsey, K. Bandy, P. P. Creasman, C. B. Griggs, C. L. Pearson, A. J. Shortland, P. Steier, High-precision dendro-^{14}C dating of two cedar wood sequences from First Intermediate Period and Middle Kingdom Egypt and a small regional climate-related ^{14}C divergence. *J. Archaeol. Sci.* **46**, 401–416 (2014).
18. S. W. Manning, C. Griggs, B. Lorentzen, C. Bronk Ramsey, D. Chivall, A. J. T. Jull, T. E. Lange, Fluctuating radiocarbon offsets observed in the southern Levant and implications for archaeological chronology debates. *Proc. Natl. Acad. Sci. U.S.A.* **115**, 6141–6146 (2018).
19. See supplementary materials.
20. C. Appenzeller, J. R. Holton, K. H. Rosenlof, Seasonal variation of mass transport across the tropopause. *J. Geophys. Res.* **101** (D10), 15071–15078 (1996).
21. A. Stohl, P. Bonasoni, P. Cristofanelli, W. Collins, J. Feichter, A. Frank, C. Forster, E. Gerasopoulos, H. Gäggeler, P. James, T. K. H. Kromp-Kolb, B. Krüger, C. Land, J. Meloen, A. Papayannis, A. Priller, P. Seibert, M. Sprenger, G. J. Roelofs, H. E. Scheel, C. Schnabel, P. Siegmund, L. Tobler, T. Trickl, H. Wernli, V. Wirth, P. Zanis, C. Zerefos, Stratosphere-troposphere exchange: A review, and what we have learned from STACCATO. *J. Geophys. Res.* **108** (D12), 8516, (2003).
22. I. Levin, T. Naegler, B. Kromer, M. Diehl, R. J. Francey, A. J. Gomez-Pelaez, L. P. Steele, D. Wagenbach, R. Weller, D. E. Worthy, Observations and modelling of the global distribution and long-term trend of atmospheric $^{14}CO_2$. *Tellus B.* **62**, 26–46 (2010).
23. C. Bronk Ramsey, M. W. Dee, J. M. Rowland, T. F. G. Higham, S. A. Harris, F. Brock, A. Quiles, E. M. Wild, E. S. Marcus, A. J. Shortland, Radiocarbon-based chronology for Dynastic Egypt. *Science* **328**, 1554–1557 (2010).
24. S. W. Manning, B. Kromer, M. W. Dee, M. Friedrich, T. F. G. Higham, C. B. Ramsey, Radiocarbon calibration in the mid to later 14th century BC and radiocarbon dating at Tell el-Amarna, Egypt, in *Radiocarbon and the Chronologies of Ancient Egypt*, A. J. Shortland, C. Bronk Ramsey, Eds. (Oxbow Books, 2013), pp. 121–145.
25. P. J. Reimer, K. A. Hughen, T. P. Guilderson, G. McCormac, M. G. L. Baillie, E. Bard, P. Barratt, J. Warren Beck, C. E. Buck, P. E. Damon, M. Friedrich, B. Kromer, C. Bronk Ramsey, R. W. Reimer, S. Remmele, J. R. Southon, M. Stuiver, J. van der Plicht, Preliminary report of the first workshop of the IntCal04 radiocarbon calibration/comparison working group. *Radiocarbon* **44**, 653–661 (2002).
26. L. McDonald, D. Chivall, D. Miles, C. Bronk Ramsey, Seasonal variations in the ^{14}C content of tree rings: Influences on radiocarbon calibration and single-year curve construction. *Radiocarbon* **61**, 185–194 (2019).
27. S. W. Manning, B. Kromer, C. Bronk Ramsey, C. L. Pearson, S. Talamo, N. Trano, J. D. Watkins, ^{14}C record and wiggle-match placement for the Anatolian (Gordion Area) juniper tree-ring chronology ~1729 to 751 cal bc, and typical Aegean/Anatolian (growing season related) regional ^{14}C offset assessment. *Radiocarbon* **52**, 1571–1597 (2010).
28. J. M. Marston, *Agricultural Sustainability and Environmental Change at Ancient Gordion* (University of Pennsylvania Museum Press, 2017).
29. O. Gordo, J. J. Sanz, Impact of climate change on plant phenology in Mediterranean ecosystems. *Glob. Chang. Biol.* **16**, 1082–1106 (2010).
30. R. M. Trigo, T. J. Osborn, J. M. Corte-Real, The North Atlantic oscillation influence on Europe: Climate impacts and associated physical mechanisms. *Climate Res.* **20**, 9–17 (2002).

31. A. Nicault, S. Alleaume, S. Brewer, M. Carrer, P. Nola, J. Guiot, Mediterranean drought fluctuation during the last 500 years based on tree-ring data. *Climate Dynam.* **31**, 227–245 (2008).
32. T. Felis, M. Ionita, N. Rimbu, G. Lohmann, M. Kölling, Mild and arid climate in the eastern sahara-arabian desert during the late little ice age. *Geophys. Res. Lett.* **45**, 7112–7119 (2018).
33. T. M. Kuster, M. Dobbertin, M. S. Günthardt-Goerg, M. Schaub, M. Arend, A phenological timetable of oak growth under experimental drought and air warming. *PLOS ONE* **9**, e89724 (2014).
34. E. E. Pflug, R. Siegwolf, N. Buchmann, M. Dobbertin, T. M. Kuster, M. S. Günthardt-Goerg, M. Arend, Growth cessation uncouples isotopic signals in leaves and tree rings of drought-exposed oak trees. *Tree Physiol.* **35**, 1095–1105 (2015).
35. N. Köse, Ü. Akkemik, H. N. Dalfes, M. S. Özeren, D. Tolunay, Tree-ring growth of *Pinus nigra* Arn. subsp. *pallasiana* under different climate conditions throughout western Anatolia. *Dendrochronologia* **30**, 295–301 (2012).
36. M. G. L. Baillie, *Tree-Ring Dating and Archaeology* (University of Chicago Press, 1982).
37. G. Helle, G. H. Schleser, Seasonal variations of stable carbon isotopes from tree-rings of *Quercus petraea*, in *TRACE. Tree Rings in Archaeology, Climatology and Ecology, Volume 1. Proceedings of the Dendrosymposium 2002, April 11th–13th 2002, Bonn/Jülich, Germany*, G. H. Schleser, M. Winiger, A. Bräuning, H. Gärtner, G. Helle, E. Jansma, B. Neuwirth, K. Treydte, Eds. (Forschungszentrum Jülich, 2003), pp. 66–70.
38. B. Kromer, S. W. Manning, M. Friedrich, S. Talamo, N. Trano, ^{14}C calibration in the 2nd and 1st millennia BC—Eastern Mediterranean Radiocarbon Comparison Project (EMRCP). *Radiocarbon* **52**, 875–886 (2010).
39. C. Bronk Ramsey, J. van der Plicht, B. Weninger, 'Wiggle matching' radiocarbon dates. *Radiocarbon* **43**, 381–389 (2001).
40. R. E. Taylor, J. Southon, Reviewing the mid-first millennium BC ^{14}C "warp" using ^{14}C/bristlecone pine data. *Nucl. Instrum. Methods Phys. Res.* **294**, 440–443 (2013).
41. A. J. Jull, I. P. Panyushkina, T. E. Lange, V. V. Kukarskih, V. S. Myglan, K. J. Clark, M. W. Salzer, G. S. Burr, S. W. Leavitt, Excursions in the ^{14}C record at A.D. 774–775 in tree rings from Russia and America. *Geophys. Res. Lett.* **41**, 3004–3010 (2014).
42. F. Miyake, A. J. T. Jull, I. P. Panyushkina, L. Wacker, M. Salzer, C. H. Baisan, T. Lange, R. Cruz, K. Masuda, T. Nakamura, Large ^{14}C excursion in 5480 BC indicates an abnormal sun in the mid-Holocene. *Proc. Natl. Acad. Sci. U.S.A.* **114**, 881–884 (2017).
43. A. Hogg, C. Turney, J. Palmer, J. Southon, B. Kromer, C. B. Ramsey, G. Boswijk, P. Fenwick, A. Noronha, R. Staff, M. Friedrich, L. Reynard, D. Guetter, L. Wacker, R. Jones, The New Zealand kauri (*Agathis Australis*) research project: A radiocarbon dating intercomparison of younger dryas wood and implications for IntCal13. *Radiocarbon* **55**, 2035–2048 (2013).
44. B. Kromer, S. Lindauer, H.-A. Synal, L. Wacker, MAMS—A new AMS facility at the Curt-Engelhorn-Centre for Archaeometry, Mannheim, Germany. *Nucl. Instrum. Methods Phys. Res.* **294**, 11–13 (2013).
45. S. Hammer, R. Friedrich, B. Kromer, A. Cherkinsky, S. J. Lehman, H. A. J. Meijer, T. Nakamura, V. Palonen, R. W. Reimer, A. M. Smith, J. R. Southon, S. Szidat, J. Turnbull, M. Uchida, Compatibility of atmospheric $^{14}CO_2$ measurements: Comparing the Heidelberg low-level counting facility to international accelerator mass spectrometry (AMS) laboratories. *Radiocarbon* **59**, 875–883 (2017).
46. S. W. Manning, C. B. Griggs, B. Lorentzen, G. Barjamovic, C. B. Ramsey, B. Kromer, E. M. Wild, Integrated tree-ring-radiocarbon high-resolution timeframe to resolve earlier second millennium BCE Mesopotamian chronology. *PLOS One* **11**, e0157144 (2016).
47. C. Tyers, J. Sidell, J. Van der Plicht, P. Marshall, G. Cook, C. Bronk Ramsey, A. Bayliss, Wiggle-matching using known-age pine from Jermyn Street, London. *Radiocarbon* **51**, 385–396 (2009).
48. A. Bayliss, P. Marshall, Confessions of a serial polygamist: The reality of radiocarbon reproducibility in archaeological samples. *Radiocarbon* **61**, 1143–1158 (2019).
49. D. Aston, Radiocarbon, wine jars and New Kingdom chronology. *Ägypten und Levante* **22–23**, 289–315 (2013).
50. I. G. Usoskin, Y. Gallet, F. Lopes, G. A. Kovaltsov, G. Hulot, Solar activity during the Holocene: The Hallstatt cycle and its consequence for grand minima and maxima. *Astron. Astrophys.* **587**, A150 (2016).
51. M. Stuiver, T. F. Braziunas, Sun, ocean, climate and atmospheric $^{14}CO_2$: An evaluation of causal and spectral relationships. *The Holocene* **3**, 289–305 (2016).
52. G. Bond, B. Kromer, J. Beer, R. Muscheler, M. N. Evans, W. Showers, S. Hoffmann, R. Lotti-Bond, I. Hajdas, G. Bonani, Persistent solar influence on North Atlantic climate during the Holocene. *Science* **294**, 2130–2136 (2001).
53. A. B. Knapp, S. W. Manning, Crisis in context: The end of the Late Bronze Age in the eastern Mediterranean. *Am. J. Archaeol.* **120**, 99–149 (2016).
54. S. W. Manning, F. Höflmayer, N. Moeller, M. W. Dee, C. B. Ramsey, D. Fleitmann, T. Higham, W. Kutschera, E. M. Wild, Dating the Thera (Santorini) eruption: Archaeological and scientific evidence supporting a high chronology. *Antiquity* **88**, 1164–1179 (2014).
55. S. W. Manning, C. B. Ramsey, W. Kutschera, T. Higham, B. Kromer, P. Steier, E. M. Wild, Chronology for the Aegean Late Bronze Age 1700-1400 B.C. *Science* **312**, 565–569 (2006).
56. F. Höflmayer, The date of the Minoan Santorini eruption: Quantifying the "Offset". *Radiocarbon* **54**, 435–448 (2012).
57. P. Warren, Archaeology: Absolute dating of the Bronze Age eruption of Thera (Santorini). *Nature* **308**, 492–493 (1984).
58. W. L. Friedrich, B. Kromer, M. Friedrich, J. Heinemeier, T. Pfeiffer, S. Talamo, Santorini eruption radiocarbon dated to 1627–1600 B.C. *Science* **312**, 548 (2006).
59. C. Bronk Ramsey, Bayesian analysis of radiocarbon dates. *Radiocarbon* **51**, 337–360 (2009).
60. I. Levin, V. Hesshaimer, Radiocarbon—A unique tracer of global carbon cycle dynamics. *Radiocarbon* **42**, 69–80 (2000).
61. J. T. Randerson, I. G. Enting, E. A. G. Schuur, K. Caldiera, I. Y. Fung, Seasonal and latitudinal variability of troposphere $\Delta^{14}CO_2$: Post bomb contributions from fossil fuels, oceans, the stratosphere, and the terrestrial biosphere. *Global Biogeochem. Cy.* **16**, 59-1–59-19 (2002).
62. I. Levin, B. Kromer, The tropospheric $^{14}CO_2$ level in mid-latitudes of the northern hemisphere (1959-2003). *Radiocarbon* **46**, 1261–1272 (2004).
63. I. Levin, J. Schuchard, B. Kromer, K. O. Münnich, The continental european suess effect. *Radiocarbon* **31**, 431–440 (1989).
64. I. Levin, B. Kromer, Twenty years of atmospheric $^{14}Co_2$ observations at Schauinsland station, Germany. *Radiocarbon* **39**, 205–218 (1997).
65. Q. Hua, M. Barbetti, Review of tropospheric bomb ^{14}C data for carbon cycle modeling and age calibration purposes. *Radiocarbon* **46**, 1273–1298 (2004).
66. F. Dellinger, W. Kutschera, K. Nicolussi, P. Schießling, P. Steier, E. Maria Wild, A ^{14}C calibration with AMS from 3500 to 3000 BC, derived from a new high-elevation stone-pine tree-ring chronology. *Radiocarbon* **46**, 969–978 (2004).
67. I. Levin, R. Bösinger, G. Bonani, R. J. Francey, B. Kromer, K. O. Münnich, M. Suter, N. B. A. Trivett, W. Wölfli, Radiocarbon in atmospheric carbon dioxide and methane: Global distribution and trends, in *Radiocarbon After Four Decades: An Interdisciplinary Perspective*, R. E. Taylor, A. Long, R. Kra, Eds. (Springer, 1992), pp. 503–518.
68. H. Kitagawa, H. Mukai, Y. Nojiri, Y. Shibata, T. Kobayashi, T. Nojiri, Seasonal and secular variations of atmospheric $^{14}Co_2$ over the western Pacific since 1994. *Radiocarbon* **46**, 901–910 (2004).
69. I. Levin, B. Kromer, M. Schmidt, H. Sartorius, A novel approach for independent budgeting of fossil fuel CO_2 over europe by $^{14}CO_2$ observations. *Geophys. Res. Lett.* **30**, 2194 (2003).
70. P. E. Damon, S. Cheng, T. W. Linick, Fine and hyperfine structure in the spectrum of secular variations of atmospheric ^{14}C. *Radiocarbon* **31**, 704–718 (1989).
71. P. E. Damon, A note concerning "Location-dependent differences in the ^{14}C content of wood" by McCormac *et al*. *Radiocarbon* **37**, 829–830 (1995).
72. P. E. Damon, G. Burr, W. J. Cain, D. J. Donahue, Anomalous 11-year Δ^{14}C cycle at high latitudes? *Radiocarbon* **34**, 235–238 (1992).
73. P. E. Damon, G. Burr, A. N. Peristykh, G. C. Jacoby, R. D. D'Arrigo, Regional radiocarbon effect due to thawing of frozen earth. *Radiocarbon* **38**, 597–602 (1996).
74. K. Suzuki, H. Sakurai, Y. Takahashi, T. Sato, S. Gunji, F. Tokanai, H. Matsuzaki, Y. Tsuchiya, Precise comparison of ^{14}C ages from Choukai jindai cedar with IntCal04 raw data. *Radiocarbon* **52**, 1599–1609 (2010).
75. W. Hong, J. H. Park, G. Park, K. S. Sung, W. K. Park, J.-G. Lee, Regional offset of radiocarbon concentration and its variation in the Korean atmosphere from AD 1650-1850. *Radiocarbon* **55**, 753–762 (2013).
76. T. Nakamura, K. Masuda, F. Miyake, K. Nagaya, T. Yoshimitsu, Radiocarbon ages of annual rings from Japanese wood: Evident age offset based on IntCal09. *Radiocarbon* **55**, 763–770 (2013).
77. S. W. Manning, B. Kromer, P. I. Kuniholm, M. W. Newton, Anatolian tree-rings and a new chronology for the east Mediterranean Bronze-Iron ages. *Science* **294**, 2532–2535 (2001).
78. Q. Hua, M. Barbetti, Influence of atmospheric circulation on regional $^{14}CO_2$ differences. *J. Geophys. Res.* **112**, D19102 (2007).
79. P. Garnsey, *Famine and Food Supply in the Greco-Roman World: Responses to Risk and Crisis* (Cambridge Univ. Press, 1988).
80. S. Isager, J. E. Skydsgaard, *Ancient Greek Agriculture: An Introduction* (Routledge, 1992).
81. M. L. West, *Hesiod, Works and Days* (Clarendon Press, 1978).
82. P. Horden, N. Purcell, *The Corrupting Sea: A Study of Mediterranean History* (Blackwell, 2000).
83. M. S. Spurr, *Arable Cultivation in Roman Italy, c. 200 B.C.–C.A.D. 100* (Society for the Promotion of Roman Studies, 1986).
84. R. Sallares, *The Ecology of the Ancient Greek World* (Duckworth, 1991).
85. P. Halstead, *Two Oxen Ahead: Pre-Mechanized Farming in the Mediterranean* (John Wiley & Sons, 2014).
86. J. Oteros, H. García-Mazo, R. Botey, A. Mestre, C. Galán, Variations in cereal crop phenology in Spain over the last twenty-six years (1986-2012). *Clim. Change* **130**, 545–558 (2015).
87. O. Borowski, *Agriculture in Iron Age Israel* (Eisenbrauns, 1987).

88. A. B. Stallsmith, Agrotika: The traditional agricultural year in the Vrokastro survey area, in *Reports on the Vrokastro Area, Eastern Crete, Vol. 2. The Settlement History of the Vrokastro Area and Related Studies*, B. J. Hayden, Ed. (University of Pennsylvania Museum of Archaeology and Anthropology, Univ. Museum Monograph, ed. 119, 2004), pp. CD–39.
89. K. D. White, *Roman Farming* (Thames and Hudson, 1970).
90. F. E. Boag, "Integrated Mediterranean farming and pastoral systems: Local knowledge and ecological infrastructure of Italian dryland farming," thesis, University of Alberta (1997); www.nlc-bnc.ca/obj/s4/f2/dsk3/ftp04/nq22954.pdf.
91. W. J. Sacks, D. Deryng, J. A. Foley, N. Ramankutty, Crop planting dates: An analysis of global patterns. *Glob. Ecol. Biogeogr.* **19**, 607–620 (2010).
92. B. Kromer, K-O. Münnich, CO_2 gas proportional counting in radiocarbon dating—Review and perspective, in *Radiocarbon After Four Decades*, R. E. Taylor, A. Long, R. S. Kra, Eds. (Springer, 1992), pp. 184–197.
93. E. M. Scott, P. Naysmith, G. T. Cook, Should archaeologists care about ^{14}C intercomparisons? why? A summary report on SIRI. *Radiocarbon* **59**, 1589–1596 (2017).
94. M. Friedrich, S. Remmele, B. Kromer, J. Hofmann, M. Spurk, K. Felix Kaiser, C. Orcel, M. Küppers, The 12,460-year Hohenheim oak and pine tree-ring chronology from central Europe—A unique annual record for radiocarbon calibration and paleoenvironmental reconstructions. *Radiocarbon* **46**, 1111–1122 (2004).
95. J. R. Pilcher, M. G. L. Baillie, B. Schmidt, B. Becker, A 7,272-year tree-ring chronology for western Europe. *Nature* **312**, 150–152 (1984).
96. K. Haneca, K. Čufar, H. Beeckman, Oaks, tree-rings and wooden cultural heritage: A review of the main characteristics and applications of oak dendrochronology in Europe. *J. Archaeol. Sci.* **36**, 1–11 (2009).
97. X. Morin, J. Roy, L. Sonié, I. Chuine, Changes in leaf phenology of three European oak species in response to experimental climate change. *New Phytol.* **186**, 900–910 (2010).
98. P. I. Kuniholm, M. W. Newton, R. F. Liebhart, Dendrochronology at Gordion, in *The New Chronology of Iron Age Gordion*, C. B. Rose, G. Darbyshire, Eds. (University of Pennsylvania Museum of Archaeology and Anthropology, 2011), pp. 79–122.
99. G. Kahveci, M. Alan, N. Köse, Distribution of juniper stands and the impact of environmental parameters on growth in the drought-stressed forest-steppe zone of central Anatolia. *Dendrobiology* **80**, 61–69 (2018).
100. L. Wacker, G. Bonani, M. Friedrich, I. Hajdas, B. Kromer, M. Němec, M. Ruff, M. Suter, H.-A. Synal, C. Vockenhuber, MICADAS: Routine and high-precision radiocarbon dating. *Radiocarbon* **52**, 252–262 (2010).
101. M. W. Dee, S. W. L. Palstra, A. T. Aerts-Bijma, M. O. Bleeker, S. de Bruijn, F. Ghebru, H. G. Jansen, M. Kuitems, D. Paul, R. R. Richie, J. J. Spriensma, A. Scifo, D. van Zonneveld, B. M. A. A. Verstappen-Dumoulin, P. Wietzes-Land, H. A. J. Meijer, Radiocarbon dating at groningen: New and updated chemical pretreatment procedures. *Radiocarbon* **62**, 63–74 (2019).
102. A. Cherkinsky, R. A. Culp, D. K. Dvoracek, J. E. Noakes, Status of the AMS facility at the University of Georgia. *Nucl. Instrum. Meth. B* **268**, 867–870 (2010).
103. J. S. Vogel, J. R. Southon, D. E. Nelson, T. A. Brown, Performance of catalytically condensed carbon for use in accelerator mass spectrometry. *Nucl. Instrum. Meth.B* **5**, 289–293 (1984).
104. P. Marshall, A. Bayliss, S. Farid, C. Tyers, C. Bronk Ramsey, G. Cook, T. Doğan, S. P. H. T. Freeman, E. İlkmen, T. Knowles, ^{14}C wiggle-matching of short tree-ring sequences from post-medieval buildings in England. *Nucl. Instrum. Meth. B* **438**, 218–226 (2019).
105. M. B. Brea, M. Cremaschi, *Acqua e Civiltà Nelle Terramare: La Vasca Votive di Noceto* (Università degli Studi di Milano, Milan, 2009).
106. F. H. Schweingruber, *Tree Rings: Basics and Applications of Dendrochronology* (D. Reidel, 1988).
107. P. W. Brewer, Data management in dendroarchaeology using Tellervo. *Radiocarbon* **56**, S79–S83 (2014).
108. K. Harris, Corina 1.1. 2007 Version of a 2003 Release; https://dendro.cornell.edu/corina/corina.php.
109. R. M. Czichon, J. Klinger, P. Hnila, D. P. Mielke, H. Böhm, C. Forster, C. Griggs, M. Kähler, G. K. Kunst, M. Lehmann, B. Lorentzen, S. Manning, K. Marklein, H. Marquardt, S. Reichmuth, J. Richter, C. Rössner, B. Sadıklar, K. Seufer, R. Sobott, I. Traub-Sobott, H. von der Osten-Woldenburg, M. Weber, H. Wolter, M. A. Yilmaz, Archäologische forschungen am oymaağaç, Höyük/Nerik 2011–2015. *Mitteilungen der Deutschen Orient-Gesellschaft zu Berlin* **148**, 5–141 (2016).
110. S. W. Manning, B. Kromer, Radiocarbon dating archaeological samples in the eastern Mediterranean, 1730 TO 1480 BC: Further exploring the atmospheric radiocarbon calibration record and the archaeological implications. *Archaeometry* **53**, 413–439 (2011).
111. S. W. Manning, B. Kromer, Considerations of the scale of radiocarbon offsets in the east Mediterranean, and considering a case for the latest (most recent) likely date for the santorini eruption. *Radiocarbon* **54**, 449–474 (2012).
112. C. Bronk Ramsey, Radiocarbon calibration and analysis of stratigraphy: The OxCal program. *Radiocarbon* **37**, 425–430 (1995).
113. C. Bronk Ramsey, Dealing with outliers and offsets in radiocarbon dating. *Radiocarbon* **51**, 1023–1045 (2009).
114. G. K. Ward, S. R. Wilson, Procedures for comparing and combining radiocarbon age determinations: A critique. *Archaeometry* **20**, 19–31 (1978).
115. T. Higham, K. Douka, R. Wood, C. B. Ramsey, F. Brock, L. Basell, M. Camps, A. Arrizabalaga, J. Baena, C. Barroso-Ruíz, C. Bergman, C. Boitard, P. Boscato, M. Caparrós, N. J. Conard, C. Draily, A. Froment, B. Galván, P. Gambassini, A. Garcia-Moreno, S. Grimaldi, P. Haesaerts, B. Holt, M.-J. Iriarte-Chiapusso, A. Jelinek, J. F. Jordá Pardo, J.-M. Maíllo-Fernández, A. Marom, J. Maroto, M. Menéndez, L. Metz, E. Morin, A. Moroni, F. Negrino, E. Panagopoulou, M. Peresani, S. Pirson, M. de la Rasilla, J. Riel-Salvatore, A. Ronchitelli, D. Santamaria, P. Semal, L. Slimak, J. Soler, N. Soler, A. Villalueng, R. Pinhasi, R. Jacobi, The timing and spatiotemporal patterning of neanderthal disappearance. *Nature* **512**, 306–309 (2014).
116. W. A. Ward, M. S. Joukowsky, *The Crisis Years: The 12th Century BC from beyond the Danube to the Tigris* (Kendall Hunt, 1992).
117. R. Drews, *The End of the Bronze Age: Changes in Warfare and the Catastrophe ca. 1200 B.C.* (Princeton Univ. Press, 1993).
118. E. H. Cline, *1177 B.C.: The Year Civilization Collapsed* (Princeton Univ. Press, 2014).
119. C. Broodbank, *The Making of the Middle Sea. A History of the Mediterranean from the Beginning to the Emergence of the Classical World* (Thames and Hudson, 2013).
120. G. D. Middleton, *Understanding Collapse: Ancient History and Modern Myths* (Cambridge Univ. Press, 2017).
121. L. Welton, T. Harrison, S. Batiuk, E. Ünlü, B. Janeway, D. Karakaya, D. Lipovitch, D. Lumb, J. Roames, Shifting networks and community identity at Tell Tayinat in the Iron I (ca. 12th to mid 10th century B.C.E.). *Am. J. Archaeol.* **123**, 291–333 (2019).
122. B. L. Drake, The Influence of climatic change on the Late Bronze Age collapse and the Greek Dark Ages. *J. Archaeol. Sci.* **39**, 1862–1870 (2012).
123. I. Neugebauer, A. Brauer, M. J. Schwab, P. Dulski, U. Frank, E. Hadzhiivanova, H. Kitagawa, T. Litt, V. Schiebel, N. Taha, N. D. Waldmann; DSDDP Scientific Party, Evidences for centennial dry periods at ~3300 and ~2800 cal. yr BP from micro-facies analyses of the Dead Sea sediments. *Holocene* **25**, 1358–1371 (2015).
124. I. Finkelstein, D. Langgut, M. Meiri, L. Sapir-Hen, Egyptian imperial economy in Canaan: Reaction to the climate crisis at the end of the Late Bronze Age. *Ägypten und Levante* **27**, 249–260 (2017).
125. M. Finné, K. Holmgren, C.-C. Shen, H.-M. Hu, M. Boyd, S. Stocker, Late Bronze Age climate change and the destruction of the Mycenaean Palace of Nestor at Pylos. *PLOS ONE* **12**, e0189447 (2017).
126. D. Kaniewski, N. Marriner, J. Bretschneider, G. Jans, C. Morhange, R. Cheddadi, T. Otto, F. Luce, E. Van Campo, 300-year drought frames Late Bronze Age to early Iron Age transition in the Near East: New palaeoecological data from Cyprus and Syria. *Reg. Environ. Change* **19**, 2287–2297 (2019).
127. W. L. Friedrich, J. Heinemeier, The Minoan eruption of Santorini radiocarbon dated to 1613 ± 13 BC—Geological and stratigraphic considerations, in *Time's Up! Dating the Minoan Eruption of Santorini*, D. A. Warburton, Ed. (The Danish Institute at Athens, 2009), pp. 57–63.
128. W. L. Friedrich, B. Kromer, M. Friedrich, J. Heinemeier, T. Pfeiffer, S. Talamo, The olive branch chronology stands irrespective of tree-ring counting. *Antiquity* **88**, 274–277 (2014).
129. J. Heinemeier, W. L. Friedrich, B. Kromer, C. Bronk Ramsey, The Minoan eruption of Santorini radiocarbon dated by an olive tree buried by the eruption, in *Time's Up! Dating the Minoan Eruption of Santorini*, D. A. Warburton, Ed. (The Danish Institute at Athens, 2009), pp. 285–293.
130. P. Cherubini, T. Humbel, H. Beeckman, H. Gärtner, D. Mannes, C. Pearson, W. Schoch, R. Tognetti, S. Lev-Yadun, Olive tree-ring problematic dating: A comparative analysis on Santorini (Greece). *PLOS ONE* **8**, e54730 (2013).
131. P. Cherubini, T. Humbel, H. Beeckman, H. Gärtner, D. Mannes, C. Pearson, W. Schoch, R. Tognetti, S. Lev-Yadun, The olive-branch dating of the Santorini eruption. *Antiquity* **88**, 267–273 (2014).
132. Y. Ehrlich, L. Regev, E. Boaretto, Radiocarbon analysis of modern olive wood raises doubts concerning a crucial piece of evidence in dating the Santorini eruption. *Sci. Rep.* **8**, 11841 (2018).
133. S. W. Manning, *A Test of Time Revisited* (Oxbow, 2014).
134. D. A. Warburton, *Time's Up! Dating the Minoan Eruption of Santorini* (The Danish Institute at Athens, 2009).
135. P. P. Betancourt, G. A. Weinstein, Carbon-14 and the beginning of the Late Bronze Age in the Aegean. *Am. J. Archaeol.* **80**, 329–348 (1976).
136. B. J. Kemp, R. S. Merrillees, *Minoan Pottery in Second Millennium Egypt* (Philipp von Zabern, 1980).
137. P. P. Betancourt, Research notes and application reports dating the Aegean Late Bronze Age with radiocarbon. *Archaeometry* **29**, 45–49 (1987).
138. S. W. Manning, *A Test of Time: The Volcano of Thera and the Chronology and History of the Aegean and East Mediterranean in the Mid-Second Millennium BC* (Oxbow, 1999).
139. C. Bronk Ramsey, S. W. Manning, M. Galimberti, Dating the volcanic eruption at Thera. *Radiocarbon* **46**, 325–344 (2004).

140. H. J. Bruins, J. Keller, A. Klügel, H. J. Kisch, I. Katra, J. van der Plicht, Tephra in caves: Distal deposits of the Minoan Santorini eruption and the Campanian super-eruption. *Quat. Int.* **499**, 135–147 (2019).
141. E. H. Cline, *Sailing the Wine-Dark Sea: International Trade and the Late Bronze Age Aegean* (BAR Int. Ser. 591, Tempus Reparatum, 1994).
142. T. Mühlenbruch, The absolute dating of the volcanic eruption of Santorini/Thera (periferia south Aegean/GR)—An alternative perspective. *Praehist. Z.* **92**, 107–192 (2017).
143. P. Warren, The date of the Late Bronze Age eruption of Santorini, in *Time's Up! Dating the Minoan Eruption of Santorini*, D. A. Warburton, Ed. (The Danish Institute at Athens, 2009), pp. 181–186.
144. M. H. Wiener, The state of the debate about the date of the Thera eruption, in *Time's Up! Dating the Minoan Eruption of Santorini*, D. A. Warburton, Ed. (The Danish Institute at Athens, 2009), pp. 197–206.
145. M. W. Salzer, M. K. Hughes, Bristlecone pine tree rings and volcanic eruptions over the last 5000 yr. *Quatern. Res.* **67**, 57–68 (2007).
146. R. K. Ritner, N. Moeller, The Ahmose 'Tempest Stela', Thera and comparative chronology. *J. Near Eastern Stud.* **73**, 1–19 (2014).
147. J. McAneney, M. Baillie, Absolute tree-ring dates for the Late Bronze Age eruptions of Aniakchak and Thera in light of a proposed revision of ice-core chronologies. *Antiquity* **93**, 99–112 (2019).
148. S. W. Manning, Events, Episodes and History: Chronology and the resolution of historical processes, in *An Age of Experiment: Classical Archaeology Transformed (1976–2014)*, L. Nevett, J. Whitley, Eds. (McDonald Institute for Archaeological Research, 2018), pp.119–137.
149. P. I. Kuniholm, Dendrochronologically dated Ottoman monuments, in *A Historical Archaeology of the Ottoman Empire: Breaking New Ground*, U. Baram, L. Carroll, Eds. (Plenum Publishers, 2000), pp. 93–136.
150. E. R. Cook, R. Seager, Y. Kushnir, K. R. Briffa, U. Büntgen, D. Frank, P. J. Krusic, W. Tegel, G. van der Schrier, L. Andreu-Hayles, M. Baillie, C. Baittinger, N. Bleicher, N. Bonde, D. Brown, M. Carrer, R. Cooper, K. Čufar, C. Dittmar, J. Esper, C. Griggs, B. Gunnarson, B. Günther, E. Gutierrez, K. Haneca, S. Helama, F. Herzig, K.-U. Heussner, J. Hofmann, P. Janda, R. Kontic, N. Köse, T. Kyncl, T. Levanič, H. Linderholm, S. Manning, T. M. Melvin, D. Miles, B. Neuwirth, K. Nicolussi, P. Nola, M. Panayotov, I. Popa, A. Rothe, K. Seftigen, A. Seim, H. Svarva, M. Svoboda, T. Thun, M. Timonen, R. Touchan, V. Trotsiuk, V. Trouet, F. Walder, T. Ważny, R. Wilson, C. Zang, Old World megadroughts and pluvials during the common era. *Sci. Adv.* **1**, e1500561 (2015).
151. C. Groves, C. Locatelli, *Tree-Ring Analysis of Conifer Timbers from 107 Jermyn Street, City of Westminster, London* (English Heritage Centre for Archaeology Report 67/2005, 2005).
152. H. Grudd, Tree-Ring Data from Mora, Sweden (Figshare Collection, 2019); https://doi.org/10.6084/m9.figshare.c.4677185.

Acknowledgments: We thank M. Friedrich for the GeO samples from the Hohenheim chronology, D. Brown for supplying the IrO samples from the Queen's University Belfast chronology, D. P. Mielke and P. Hnila for the samples from OYM and sharing ^{14}C dates on these and for collaboration on this material, and H. Grudd for supplying dendrochronologically dated Swedish pine. We thank C. Kocik and B. Lorentzen for work on the NOC and OYM tree ring samples. We thank M. Baillie for advice on IrOs. We thank the three referees for helpful and constructive comments. We acknowledge the Italian Ministry of Cultural Heritage and Activities (MiBAC) and the Municipality of NOC for supporting the archaeological excavation of the site. This work is part of the activities supported by the Italian Ministry of Education, University and Research (MIUR) through the project "Dipartimenti di Eccellenza 2018–2022" awarded to the Dipartimento di Scienze della Terra "Ardito Desio" of the Università degli Studi di Milano. **Funding:** This work was supported by the NSF (award no. BCS 1219315); the Social Science and Humanities Research Council, Canada, via the CRANE project, University of Toronto (award no. 895-2011-1026); and the College of Arts and Sciences and the Department of Classics, Cornell University. The research of M.W.D. is supported by an ERC grant (714679, ECHOES). The investigation at NOC was funded in the framework of the SUCCESSO-TERRA Project, financed by MIUR (grant no. PRIN20158KBLNB, P.I. to M.C.). **Author contributions:** S.W.M. and B.K. designed the study. B.K., M.W.D., R.F., and C.S.H. carried out ^{14}C dating. C.G., S.W.M., and M.C. worked on dendrochronology. S.W.M. drafted the manuscript with additional inputs from all coauthors. **Competing interests:** The authors declare that they have no competing interests. **Data and materials availability:** All data needed to evaluate the conclusions in the paper are present in the paper and/or the Supplementary Materials. Additional data related to this paper may be requested from the authors.

Submitted 13 August 2019
Accepted 19 December 2019
Published 18 March 2020
10.1126/sciadv.aaz1096

Citation: S. W. Manning, B. Kromer, M. Cremaschi, M. W. Dee, R. Friedrich, C. Griggs, C. S. Hadden, Mediterranean radiocarbon offsets and calendar dates for prehistory. *Sci. Adv.* **6**, eaaz1096 (2020).